BEHAVIOR RESPONSE OF AN ALPINE LAKE COPEPOD TO THIN LAYER STRUCTURE

A Thesis
Presented to
The Academic Faculty

by

Anna Skipper

In Partial Fulfillment
of the Requirements for the Degree
Master of Science in the
School of Civil and Environmental Engineering

Georgia Institute of Technology
December 2016

BEHAVIOR RESPONSE OF AN ALPINE LAKE COPEPOD TO THIN LAYER STRUCTURE

Approved by:

Dr. Donald R. Webster, Advisor
School of Civil and Environmental Engineering
Georgia Institute of Technology

Dr. Marc Weissburg
School of Biology
Georgia Institute of Technology

Dr. Jeannette Yen
School of Biology
Georgia Institute of Technology

Date Approved: October 11, 2016

ACKNOWLEDGEMENTS

Thanks to all the labmates, past and present: Aaron True, David Young, and John Jung. Aaron in particular, thanks for doing a ton of work during your own time here to make this masters thesis more approachable. Also thanks for always making time to be available for my questions! David, thanks for answering random MATLAB questions, arranging lab get-togethers, and reluctantly providing copepod-related advice. John, thanks for being the most even-tempered member of the lab-group and for being my homework partner. The lab isn't the same without you, buddy!

Thanks to Dr. Yen for collecting the copepods and her help along the way. Thanks also to her lab, especially Larissa, for taking care of the copepods and answering my questions.

Thanks to Geries Abuakel for emotional support and library company through the worst of the thesis-making process. It was a good trial run for the next adventure.

Thanks to friends and family for always keeping it real and providing perspective.

Thanks to the Office of Naval Research for funding this work.

TABLE OF CONTENTS

LIST OF TABLES

LIST OF FIGURES

SUMMARY

The objective of this study is to determine for the alpine copepod *Hesperodiaptomus shoshone* whether a) the species responds to hydromechanical cues in a manner similar to marine copepods, and b) if shear strain rate is an important cue in mating behavior. The study isolates the response of the freshwater copepod to the hydromechanical cue of shear strain rate by exposing it to a flow structure similar to that of a thin layer shear flow, which is a vertically thin, horizontally expansive region of high productivity found in nearly all marine environments. While the behavior of marine copepods in and around the hydrodynamic cues associated with thin layers have been studied, very little work has been done to date investigating whether freshwater species exhibit similar behavior responses. In addition, the hydromechanical cues of velocity gradients and shear strain rates have been shown to help other species of copepods to locate mates.

A free shear flow was simulated in the laboratory by creating laminar, planar free jet (the Bickley jet) in a recirculating system. This system is set up to mimic the fine-scale hydrodynamic structure of a horizontal shear layer. The magnitudes of shear strain rates in this system are also similar to synthetic trails used in mate-following experiments. Eight bioassays were conducted: 2 male controls (stagnant water), 2 male treatments (planar jet), 2 female controls, and 2 female treatments.

The freshwater copepod, *H. shoshone*, (both males and females) exhibited a treatment effect in each kinematic parameter except turning frequency in the in-layer vs. out-of-layer (location) analyses. *H. shoshone* decreased its relative swimming speed (mm/s and $bodylengths/s$) from control to treatment in both the location and exposure analyses, which is consistent with a corresponding increase in the proportional

vicinity time. Significant differences between sexes were observed in turning frequency, with females turning more than males. This result is consistent with a lower net-to-gross displacement ratio, which indicates curvier paths, for the females compared to the males. However, it is important to note that none of the kinematic parameters yielded an effect due to the copepods' location or exposure. In addition, there was no interaction between the treatment effect and the location or exposure effect. Such global responses are difficult to interpret as direct responses to the presence of the layer without a corresponding dependence on the layer region.

In contrast, a physiologically-similar marine copepod, *Calanus finmarchicus*, has been shown previously to react strongly to the presence of thin layer cues via increased swimming speed, increased turn frequency, and increased residence time (Woodson et al. 2007b). The contrasting behavior may be due to fundamental differences in environment and ecology. Thin layer structure rarely appears in alpine lakes, which are typically shallow and mix vertically often and rapidly. In contrast, thin layers are persistent, stable features in marine environments that have been observed throughout the worlds oceans. For the marine species, the velocity gradient cue ranks in a cue hierarchy that indicates to the animals where food and mates might be found. In this freshwater species, however, there seems to be no association among flow structure, food, and mates.

CHAPTER I

INTRODUCTION

Thin layers are vertically thin, horizontally expansive layers of high productivity that are found in nearly all marine environments (McManus et al. 2003). In these regions, individual behavioral processes at the fine scale ($< 1m$) can be linked to submesoscale ($10 - 100m$) processes (e.g., plankton density) that dictate marine productivity. For this reason, the behavior of marine zooplankton around thin layer structure has been a recent area of much research (McManus et al. 2003; Woodson et al. 2007b; Woodson et al. 2007a; True 2014). These studies have found that many marine copepods respond to isolated cues that correspond to thin layer cues, such as velocity gradients and chemical exudates (Woodson et al. 2007b), as well as exhibit species-specific responses to combined cues that represent a cue hierarchy, in which velocity gradients initially narrow search regions and chemical cues and food presence cause changes in behavior (Woodson et al. 2007a; Woodson et al. 2007b). The responses of the copepods examined in these studies included increased swimming speed, increased turning frequency, and/or increased time spent within the thin layer mimic which was the same apparatus in both cases.

Just as in marine ecosystems, freshwater zooplankton serve as the link between primary producers like phytoplankton to those animals higher in the food chain (Mauchline 1998). However, little has been done to investigate whether freshwater zooplankton exhibit the same type of behavior around thin layer flow structures, or flow structure in general. This gap in understanding in freshwater ecosystems is a hindrance in studying lakes as "sentinels of climate change" as a recent study has suggested (Adrian et al. 2009). Adrian et al. (2009) states that biota (plants and

animals) can be used as an indicator to measure the effects of climate change in lakes by looking at invaders of specific communities and other changes in community structure. Because zooplankton are often documented over long periods of time, declines (or inclines) in certain populations could be more easily detected.

While lakes in general are well-suited towards climate change studies due to the rapid turnover from organismal to ecosystem scales in these environments (Adrian et al. 2009), alpine lakes have been shown to be even more sensitive to climate change (Parker et al. 2008). In general, high-altitude environments are more rapidly affected by climate change due to the increase of ultraviolet radiation (UVR) flux with increases in elevation (Sommaruga 2001) and the lower reflectivity of alpine lakes (Slaymaker 1979). In addition, alpine lakes have relatively simple food webs (Sprules 1972), which makes changes in community structure more detectable, and are removed from local sources of pollution and direct human influence (Sommaruga 2001), which makes them candidates for more broad climate change studies.

One direct effect of climate change in alpine region are changes in snow pack; during years of low snow pack, *Hesperodiaptomus shoshone*, a freshwater alpine copepod, has been shown to invade other ponds, while during years of high snow pack, their own ponds are invaded (Williams 2012). This correlation makes *H. shoshone* an interesting candidate as an indicator organism for climate change in alpine lakes. Like many other organisms in alpine lakes, *H. shoshone* has UVR protection in the form of a bright red pigment. Therefore, the changes in UVR in alpine ecosystems could be reflected in either physical (e.g., darkening of pigment) or behavioral changes (e.g., increased daytime surface avoidance) in *H. shoshone*. This animal has also been found to thrive during warmer years (or in warmer lakes) due to the increase of swimming speed with temperature (up to 16°C), which corresponds to increased successful mating encounters (Kramer et al. 2011).

Recent studies have focused on the mating behavior of *H shoshone*. Understanding

mating behavior is a crucial aspect of quantifying the population dynamics of a species - especially in one like *H. shoshone* that has few natural predators in its habitat. Achieving critical density - the density of a species below which population growth rates are negative - is a major problem for copepods, that can be separated by 100's of body lengths. Such animals can achieve greater mating success by rapid swimming as well as pheromone trail following (Kramer et al. 2011). Previously only seen in marine species of copepods, *H. shoshone* was the first freshwater copepod discovered to exhibit trail following behavior (Yen et al. 2011).

However, the way the pheromone trail mimics are created in the laboratory requires the presence of multiple cues. The water is dosed with female pheromone scent and weighted with Dextran, a high-weight molecular sugar, which caused the trail to fall; the edges of the trail create a strain rate as the higher velocity of the trail jet pulls on the stagnant fluid to either side, causing a fluid mechanical cue as well (Yen et al. 2011). Pender-Healy (2014) has found that *H. shoshone males* follow scented as well as scentless trails. If indeed this animal uses both chemical and hydromechanical cues to track its mates, it would be the first species ever discovered to do so.

Therefore the current study seeks to isolate the fluid mechanical cue from other cues present in the pheromone trails in order to determine whether this is the relevant cue in the trail following experiments.

CHAPTER II

LITERATURE REVIEW

This chapter reviews literature on free shear flows, with particular emphasis on thin layers and the Bickley jet; mechanosensing abilities in zooplankton; and two species of calanoid copepods (crustacean zooplankton), *Hesperodiaptomus shoshone* and *Calanus finmarchicus*. First, the theoretical framework behind free shear flows is discussed as well as the importance of these flows in environmental fluid mechanics. The two free shear flows of particular interest in this study, thin layers and the Bickley jet, are discussed in greater detail. Next, mechanosensing is reviewed, and the relevant fluid mechanical parameters are defined. Finally, a brief overview of calanoid copepods is given, contextualizing their role in aquatic communities and ecosystems. Both *H. shoshone* and *C. finmarchicus* are then examined more closely, focusing on their respective environments and ecologies as well as previous studies concerning the behavior of these animals.

2.1 Free Shear Flows

Free shear flows, so named due to the lack of fixed or solid boundaries, are flows in which fluid particles move mostly parallel to each other and grow with distance downstream. Common examples of free shear flows include fluid body intrusions (approximated by plane jets), wakes behind solid objects, and mixing layers, as depicted in Figure 2.1 (Kundu et al. 2012). There are no fixed boundaries, only interfaces (outlined) between low (e.g., wake and mixing layer) or zero (e.g., jet) fluid velocity regions and higher fluid velocity regions. In all three cases, the dominant flow is in the x (streamwise) direction and the mean velocity profiles vary most strongly in the y (transverse) direction.

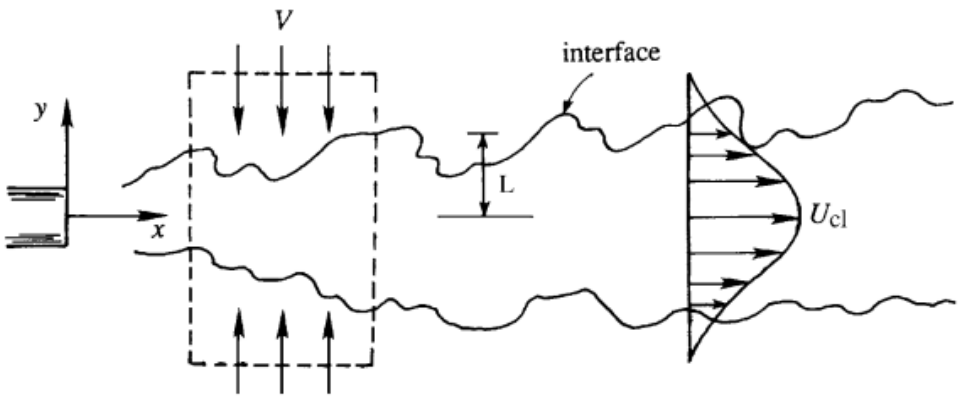

(a) Jet

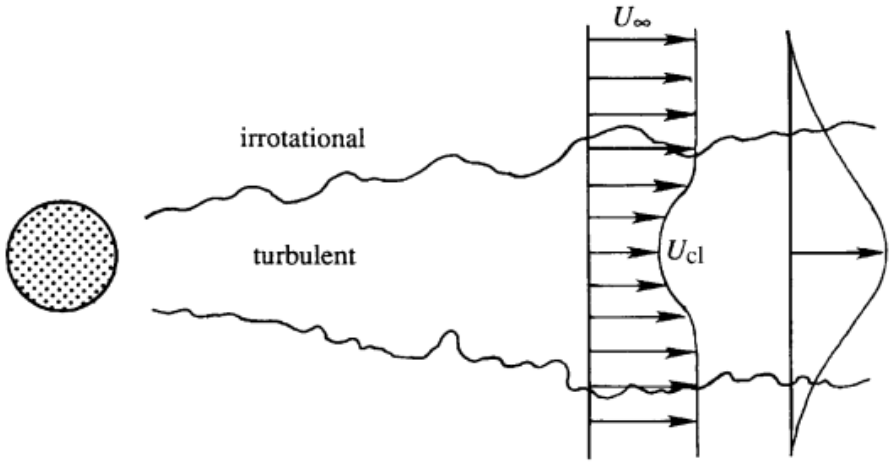

(b) Wake

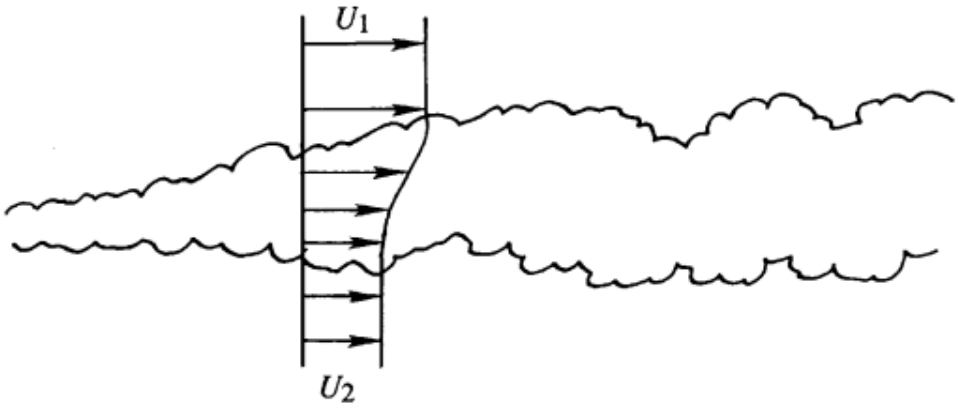

(c) Mixing Layer

Figure 2.1: Examples of free shear flows (Kundu et al. 2012)

Though ordinarily turbulent, the mean profiles (e.g., velocity, concentration) of shear flows are smooth functions that are often self-similar when scaled appropriately, as well as self-preserving. This means that profile shapes, mean and turbulent, are determined only by local scales of length and velocity.

The two types of shear flows of interest in this study are thin layers and the Bickley jet (see Figure 2.1a).

2.1.1 Thin Layers

Thin layers are vertically thin ($\sim$1 m) layers in the ocean with relatively large horizontal spans ($\sim$1 km^2) in which biomass is several order of magnitude higher than in the regions above and below (McManus et al. 2003). These regions of enhanced productivity have a profound impact on the health and vitality of marine ecosystems. Most importantly, thin layers are regions in which individual behavioral processes at the fine scale ($<$1 m) can be linked to submesoscale ($10 - 100m$) processes (e.g., plankton density) that dictate marine productivity.

Thin layers are found in nearly all marine environments (e.g., fjords, river mouths, continental shelves) and are nearly always formed at the pycnolcline, the region in which the density gradient is the greatest (McManus et al. 2003). Because of this, the Richardson number (Ri), the ratio of the stabilizing force of stratification to the destabilizing force of vertical shear, is used to determined whether thin layers are likely to form given *in-situ* conditions. Field studies have determined that the condition $Ri > 0.25$ must be met in order for thin layers to form (McManus et al. 2003; Dekshenieks et al. 2001). This number is in fact the critical value of Ri given by the normal linear stability analysis of continuous stratification with vertical shear (Drazin and Reid 1981). Therefore we see that in order for thin layers to form, turbulent mixing must be suppressed and stratification maintained. Various formation mechanisms have been proposed, both mechanical and biological in nature (see Cheriton et al.

2009). Here, however, we are most concerned with the generation of vertical shear, which could be induced by current jets, the passage of internal waves, or fluid body intrusions (Franks 1995; Ryan et al. 2008).

In marine environments, mobile plankton have been observed to aggregate in response to mechanical (as well as chemical) cues associated with thin layers (Woodson et al. 2005; Woodson et al. 2007a). In these studies, the mechanical cues were generated by a free shear flow. This type of a flow is appropriate for laboratory studies because of the association of thin layer formation in conjunction with the pycnocline, which essentially marks the interface between two layers. Similarly, True et al. (2015) has recently investigated fine-scale upwelling and downwelling shear flows, which are vertically oriented shear flows with horizontal gradients of velocity.

2.1.2 The Bickley Jet

The Bickley jet is a laminar planar jet with known analytical solutions. The analysis, credited to Bickley (1937), proceeds as follows.

We consider a steady, incompressible flow generated by a viscous jet, issuing from a long, narrow orifice into a stagnant fluid body. We take the Prandtl boundary layer equations as a good approximation to a planar jet. Using order of magnitude arguments, we can justify that the pressure is invariant in the x (streamwise) direction and y (transverse) direction and that only the y diffusion term matters. Therefore the continuity and x-momentum equations become

$$\frac{\partial u}{\partial x} + \frac{\partial v}{\partial y} = 0 \tag{2.1}$$

$$u\frac{\partial u}{\partial x} + v\frac{\partial u}{\partial y} = \nu\frac{\partial^2 u}{\partial y^2} \tag{2.2}$$

where u and v are the horizontal and vertical components of velocity respectively and ν is the kinematic viscosity. The flow is also subject to the following boundary

conditions:

$$\frac{\partial u}{\partial y} = 0 \text{ at } y = 0 \tag{2.3}$$

$$v = 0 \text{ at } y = 0 \tag{2.4}$$

$$u \to 0 \text{ as } y \to \infty \tag{2.5}$$

In addition, the momentum flux is conserved such that

$$M = \int_{-\infty}^{\infty} u^2 dy = M_0 \tag{2.6}$$

where M_0 is the initial momentum flux.

The final flow solution (form reported by Sato and Sakao 1964) is:

$$\frac{u}{U_0} = sech^2\left(\frac{ay}{\delta}\right) \tag{2.7}$$

where $a = 0.88136$ and is an experimental constant (Andrade 1939; Sato and Sakao 1964), U_0 is the maximum (centerline) velocity,

$$U_0 = \left(\frac{3M^2}{32\nu x}\right)^{1/3} \tag{2.8}$$

and δ is the half-width of the jet,

$$\delta = a\left(\frac{48\nu^2 x^2}{M}\right)^{1/3} \tag{2.9}$$

The centerline velocity at $x = 0$ is clearly singular, which has given rise to the idea of a virtual origin some distance upstream of the nozzle as the location of a point source of momentum in order to account for the non-zero nozzle width (Andrade 1939).

This jet is notoriously difficult to set up in a laboratory (Andrade 1939; Sato and Sakao 1964) as it is unstable at low Reynolds numbers. Woodson et al. (2005; 2007b) successfully implemented a laboratory scale realization of a Bickley jet to conduct copepod behavioral assays. This same apparatus was used by True (2014) to better quantify the flow field using planar particle image velocimetry (PIV). In Figure 2.2, we can see that there is good agreement between the PIV data (Figure 2.2a) and the theoretical solution (Figure 2.2b).

2.2 Mechanosensing

Zooplankton, like all other animals, depend on their senses to navigate and interact with the environment around them. One such sense exhibited by zooplankton is mechanosensing (Yen et al. 1992), which is the ability of an animal to recognize and respond to fluid mechanical cues. Within any flow field there are several cues that an animal might be able to detect, including acceleration, vorticity, and deformation rate (Kiørboe and Visser 1999).

Any three-dimensional velocity gradient, $\frac{\partial u_i}{\partial x_j}$, can be decomposed into a rotational part (rotation tensor r_{ij}) and an irrotational part (strain rate tensor e_{ij}), where i and j are the three coordinate directions, as shown in Equation 2.10.

$$\frac{\partial u_i}{\partial x_j} = e_{ij} + \frac{1}{2} r_{ij} \tag{2.10}$$

The strain rate tensor (e_{ij}), which denotes pure deformation, is given by

$$e_{ij} = \frac{1}{2}\left(\frac{\partial u_i}{\partial x_j} + \frac{\partial u_j}{\partial x_i}\right) = \begin{vmatrix} \frac{\partial u_1}{\partial x_1} & \frac{1}{2}\left(\frac{\partial u_2}{\partial x_1} + \frac{\partial u_1}{\partial x_2}\right) & \frac{1}{2}\left(\frac{\partial u_3}{\partial x_1} + \frac{\partial u_1}{\partial x_3}\right) \\ \frac{1}{2}\left(\frac{\partial u_2}{\partial x_1} + \frac{\partial u_1}{\partial x_2}\right) & \frac{\partial u_2}{\partial x_2} & \frac{1}{2}\left(\frac{\partial u_3}{\partial x_2} + \frac{\partial u_2}{\partial x_3}\right) \\ \frac{1}{2}\left(\frac{\partial u_3}{\partial x_1} + \frac{\partial u_1}{\partial x_3}\right) & \frac{1}{2}\left(\frac{\partial u_2}{\partial x_3} + \frac{\partial u_3}{\partial x_2}\right) & \frac{\partial u_3}{\partial x_3} \end{vmatrix} \tag{2.11}$$

and the rotation tensor (r_{ij}), which denotes relative velocity due to fluid rotation (i.e., vorticity), is given by

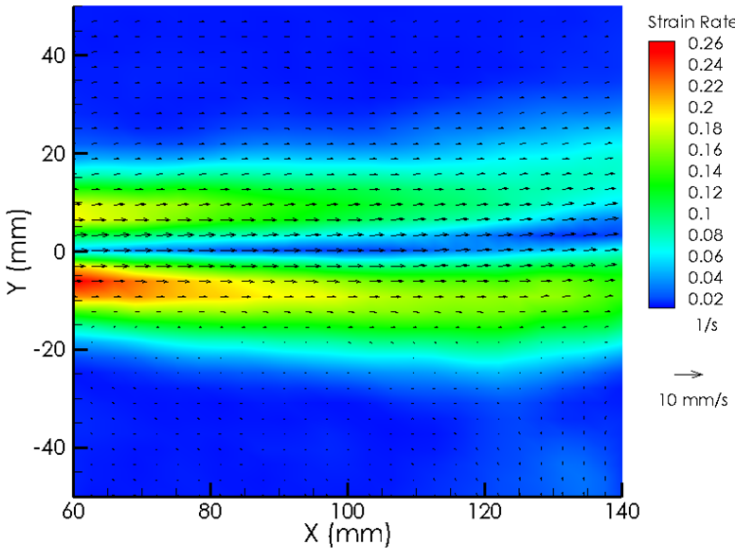

(a) PIV results

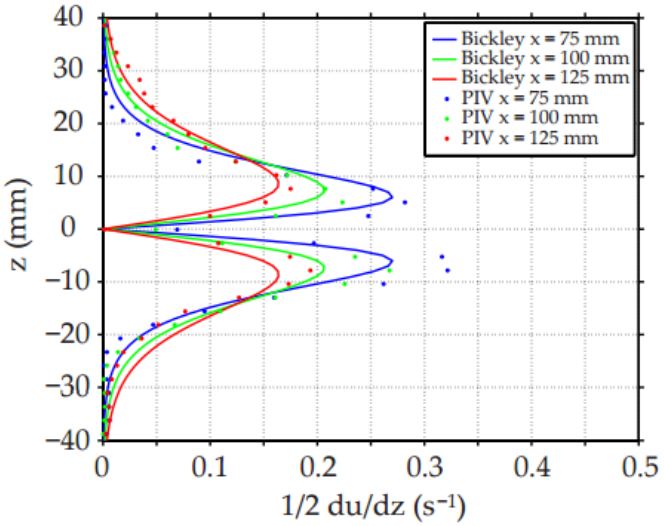

(b) Comparison with theoretical

Figure 2.2: Laboratory realization of a Bickley jet, $Re_j \sim 50$ (True 2014)

$$r_{ij} = \frac{\partial u_i}{\partial x_j} - \frac{\partial u_j}{\partial x_i} = -\varepsilon_{ij}\omega_k = \begin{vmatrix} 0 & -\left(\frac{\partial u_2}{\partial x_1} - \frac{\partial u_1}{\partial x_2}\right) & -\left(\frac{\partial u_3}{\partial x_1} - \frac{\partial u_1}{\partial x_3}\right) \\ \left(\frac{\partial u_2}{\partial x_1} - \frac{\partial u_1}{\partial x_2}\right) & 0 & -\left(\frac{\partial u_3}{\partial x_2} - \frac{\partial u_2}{\partial x_3}\right) \\ \left(\frac{\partial u_3}{\partial x_1} - \frac{\partial u_1}{\partial x_3}\right) & \left(\frac{\partial u_2}{\partial x_3} - \frac{\partial u_3}{\partial x_2}\right) & 0 \end{vmatrix} \quad (2.12)$$

The strain rate tensor can be further decomposed into normal strain rate terms, located on the diagonal (e.g., $\frac{\partial u_1}{\partial x_1}$), and shear strain rate terms (e.g., $\frac{1}{2}\left(\frac{\partial u_2}{\partial x_1} + \frac{\partial u_1}{\partial x_2}\right)$).

Mechanosensing is believed to allow zooplankton to distinguish among types of flow of interest to them – to be able to tell the difference between the suction force from a predator (Holzman and Wainwright 2009) and the wake signature of a potential mate (van Duren 1998). Copepods, as well as other crustacean zooplankton, are able to sense such spatial gradients of flow via their setae, an array of mechanosensory hairs, which are most concentrated at the antennules (Yen and Fields 1992; Fields et al. 2002). Bending or deformation of setae have been shown to generate neural signals (Fields et al. 2002); therefore the fluid motion must be relative to the copepod to bend the setae and to elicit a behavioral response.

Yen et al. (1992) determined that very small displacements ($\sim$10 nm) can cause a neural response, with velocities as small as 20 $\mu m/s$. These setae allow copepods to detect closely spaced stimuli, though their response is dependent on stimuli frequency and duration. However, Yen and Fields [1992], Kiørboe and Visser (1999), and Kiørboe et al. (1999) found that for copepods, deformation rate, not velocity, was the relevant fluid mechanical cue that induced an escape response. Threshold escape responses ranged from 1.19 to 2.49s^{-1} (Woodson et al. 2014).

Setae can also supply directional information, as shown by Strickler and Balazsi (2007) who found that copepods could distinguish the source of a hydrodynamic disturbance based on the information contained in the signal. Other behavioral responses exhibited by zooplankton are increased turn frequency and swimming speed consistent with area-restricted foraging behavior, as shown by Woodson et al. (2005). In this experiment,in which copepods were exposed to a laboratory mimic of a thin layer shear flowm species-specific behavioral strain rate thresholds ranged from 0.015 to 0.06 s^{-1} for copepods *Acartia tonsa* and *Temora longicornis*. Behavioral responses will be affected by animal size and setal sensitivity (Kiørboe et al. 1999) as well as

body orientation with respect to the signal(Fields 2010). Jiang et al. (2009) indicates that it is important that the fluid mechanical signal is resolved at the setal location.

2.3 Calanoid Copepods

Zooplankton are a diverse group of aquatic animals, of which copepods (sub-Class Copepoda, phylum Crustacea) are only a subset. However, copepods are likely the most prolific multi-cellular organisms on Earth, outnumbering even insects (Mauchline 1998). Calanoid copepods (of the Order Calanoida) live mostly in marine environments (∼75%) within the pelagic zone, where they serve as the link between phytoplankton and those organisms higher in the food chain. As illustrated in Figure 2.3, these animals typically exhibit one of four types of swimming behavior: cruising, cruise and sink, hop and sink, or jumping.

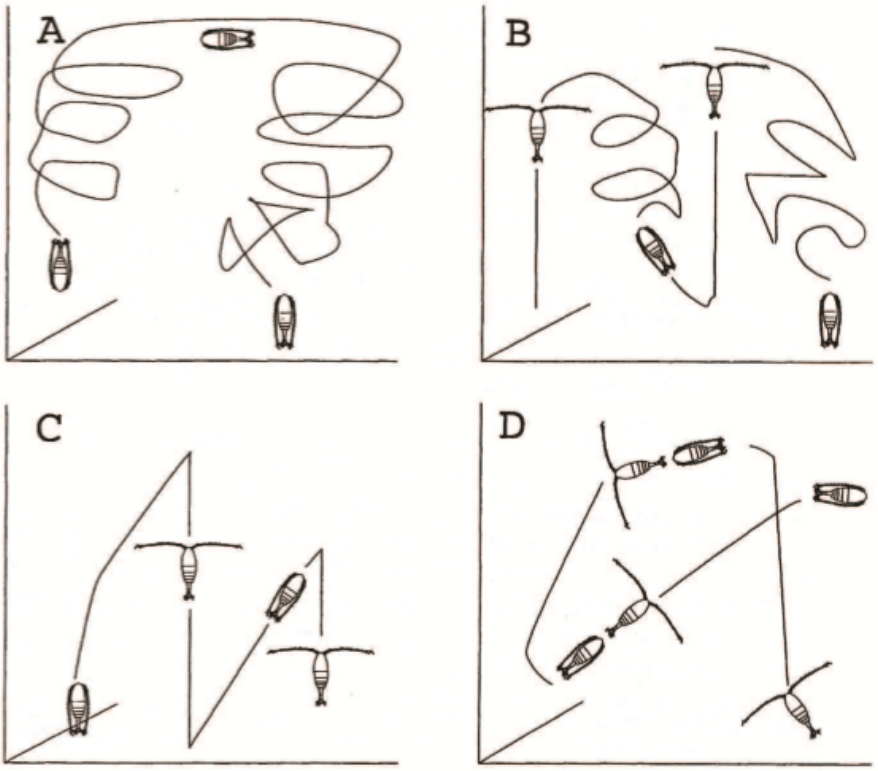

Figure 2.3: Swimming styles of calanoid copepods: (a)cruise, (b)cruise and sink, (c)hop and sink, and (d)jumping (Mauchline 1998)

All calanoid copepod species go through a similar life cycle: they hatch from eggs, then pass through a series of larval stages, and finally enter the adult stage. (Mauchline 1998)

In the sections below, two species of calanoid copepods, freshwater *H. shoshone* and marine *C. finmarchicus*, will be reviewed in more detail. Their respective environments and ecology is examined, and then the relevant literature regarding their behavior is reported.

2.3.1 *Hesperodiaptomus shoshone*

2.3.1.1 Environment and Ecology

Hesperodiaptomus shoshone (Family Diaptomidae), depicted in Figure 2.4, are large copepods ($\sim 3-4$ mm) found in alpine lakes and ponds in the mountain ranges of the United States and Canada (Yen, personal communication).

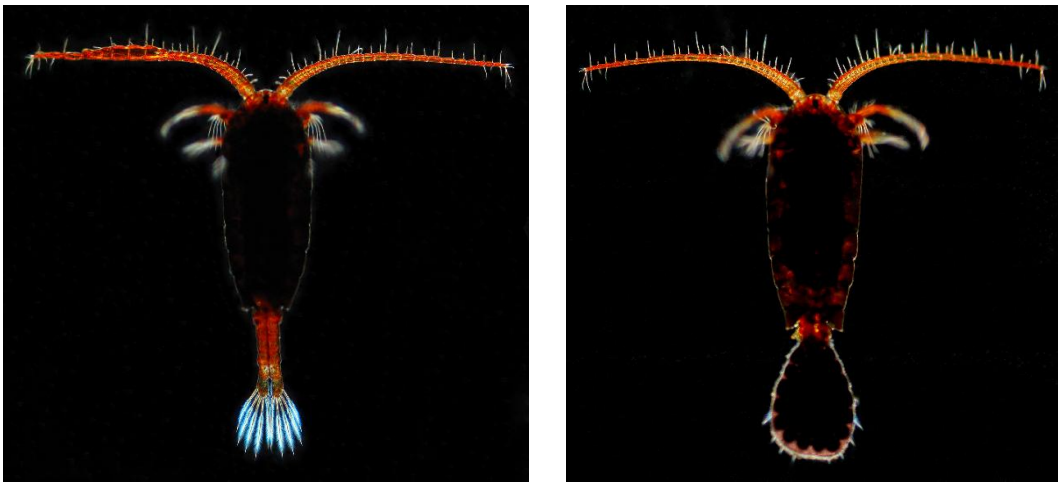

(a) Male (3.44 *mm*) (b) Female (3.72 *mm*), with eggs

Figure 2.4: Photographic image of *Hesperodiaptomus shoshone*, (a)male and (b)female (photo from Gardiner 2010)

Alpine climates are usually located in young fold mountain belts. This environment is generally characterized by high radiant energy; high moisture fluxes; discharge hydrographs greatly influenced by snowmelt and glacier melt; high available relief (or a large difference between the highest and lowest points in the area); poorly developed

regolith, the loose layer of rock over bedrock; and low percentage of ground cover by trees and other vegetation. (Slaymaker 1979)

Lakes in these regions are classified according to seasonal temperature changes (or lack thereof). These classifications are (1) temperate, where the surface temperature of the lake is greater than 4°C in summer and less than 4°C in winter; (2) subpolar, where the surface temperature is greater than 4°C for only a short period during the summer; and (3) polar, where the surface temperature is always less than 4°C. (Slaymaker 1979)

Alpine lakes are usually very clear due to low influx of sediments, with an albedo of approximately 5%, though glacier fed lakes have higher sediment content and therefore higher albedo ($15 - 20$ %) (Hutchinson 1957). Due to this low reflectivity in alpine lakes, in addition to higher fluxes of UVR at high altitudes, alpine aquatic organisms have adapted several strategies in order to minimize UVR damage (Sommaruga 2001). Copepods in alpine lakes often accumlate high levels of carotenoids that give them their "characteristic" red color (Sommaruga 2001), as shown for *H. shoshone* in Figure 2.4. Carotenoids, the pigments that give sweet potatoes and kale their vibrant colors, do not directly absorb UVR; rather, these pigments reduce the effects of radical oxygen species that can cause cellular damage. There seems to be a metabolic cost to maintaining these carotenoids: pigment levels for copepods were dramatically reduced when copepods were removed from UVR exposure (Hansson et al. 2007).

Typically, *H. shoshone* are abundant in shallow, hard-bottomed, subpolar lakes and ponds. Subpolar lakes generally have small thermal gradients and a poorly developed thermocline that is located near the surface (Hutchinson 1957). This is very different from a typical lake, which will have an epilimnion (upper layer), above the thermocline (midlimnion), underneath which will lie the hypolimnion (Fischer et al. 1979). Like most lakes, subpolar lakes have two main circulation periods, but unlike a typical lake, they occur in early summer and early autumn (rather the spring

and autumn). During the summer period, however, the lakes will mix very often due to rapid overnight cooling of the surface layer (Hutchinson 1957). The shallowness of the lakes causes the lakes to mix even more frequently, since even a light breeze will cause mixing over the entire depth. Because these lakes are shallow, they freeze completely during the winter and sometimes dry up in summer, creating a hard bottom rather than the soft mud layer seen in deeper waters

Despite a markedly higher abundance in shallow regimes, *H. shoshone* can survive in isolation in deeper waters (Sprules 1972). However, though highly dispersive, *H. shoshone* do not invade deeper ponds because once there they are heavily preyed upon by other species (Williams 2012; Sprules 1972). These predators are restricted to the deeper ponds due to physical conditions: the larvae of these species (e.g. *Chaoborus americanus* and *Ambystoma tigrinum* axolotl) cannot survive the winters in shallow lakes, during which the entire lake freezes. Within the shallow lakes, however, *H. shoshone* is a top predator, though food webs in these communities are often extremely simple (Sprules 1972). In addition, Williams (2012) conducted a long-term study in alpine ponds of the Beartooth Mountains range in Wyoming that concurred with these results, showing that extreme events of low or high snowmelt resulted in a "switch" in dominance within alpine ponds to *H. shoshone* or *C. americanus* respectively.

2.3.1.2 Behavior

H. shoshone are cruise swimmers (see Figure 2.3(a)), meaning they swim continuously. This type of swimming, often called "slow swimming" involves gliding, looping, and swimming in circles, both upwards and downwards, usually in a smooth motion (Mauchline 1998).

Pennak (1944) reported that like marine copepods, *H. shoshone* also exhibits diurnal migrations, moving towards the surface of the lake near sunset (∼6 PM) and diving back towards the bottom near sunrise (∼5 AM). The timing indicates that

this is a phototactic response rather than initiated by a mechanical or chemical cue. However, since there are few natural predators of *H. shoshone* in their home ponds, this diurnal migration is most likely due to UVR avoidance (Kessler et al. 2008) rather than predator-avoidance as is seen in marine animals (Enright and Hamner 1967).

Interestingly, the two sexes exhibited slightly different behaviors in this migration: the males tended to move upwards more and at a faster rate, with increased upward mobility after the first initial "rush" at sunset. Meanwhile, the females actually exhibited a slight downward movement shortly after the initial upwards migration (Pennak 1944). The observations are further supported by Maly (1970), who while sampling at three different depths ("Top," "Middle," and "Bottom") in 5 different alpine ponds recorded higher numbers of males in the upper regions and higher numbers of females in the lower regions. These samples were taken between 8 AM and 9 PM; and in all cases, the total number of males collected exceeded the total number of females collected ($53 - 77\%$).

Maly (1978) reported that *H. shoshone* collected from a pond without extensive predation showed differences in mean size between males ($1.52 \pm 0.09\ mm$) and females ($1.71 \pm 0.11\ mm$). The male distribution was truncated for smaller values than its mean, whereas the female distribution was truncated for larger values than its mean. In addition, larger males (1.65 mm) tended to mate with larger females (1.85 mm), who were also more likely to have spermatophores (i.e., capsules of male reproductive material), indicating that "it is good to be a large [*H. shoshone*] in this study pond."

This bias towards larger mates could reflect an evolutionary drive to increase the critical population density, or the density of copepods below which population growth rates are negative. Kramer et al. (2011) indicated that the critical density was highly dependent on male swimming speed as well as body size, since larger body sizes favor the production of pheromone trails. These animals (males) have

demonstrated the ability to detect and follow pheromone trails of females as well as female-scented trail mimics, and they are the first freshwater species discovered to do so (Yen et al. 2011). Pender-Healy (2014) showed that males of this species also follow scent-less trails as well as male-scented trails, which could indicate that these animals utilize hydromechanical cues as well as chemical cues in mate detection and capture. This type of behavior has not been seen in copepods before and therefore requires further investigation. Another freshwater calanoid copepod, *Leptodiaptomus ashlandi*, was found to advect female scent through a feeding current rather than by following their mates directly. The animals increased their swimming speed in response to the presence of female scent (Nihongi et al. 2004).

2.3.2 *Calanus finmarchicus*

Calanus finmarchicus (Family Caladinae),depicted in Figure 2.5 is a key species of large copepods ($\sim 3-4$ mm) that live in the North Atlantic Ocean. Because *C. finmarchicus* is one of the most studied animals, there is a vast body of literature on this species. However, I will only briefly review a few topics of interest to this study.

C. finmarchicus are often the dominant large copepod in high latitude marine environments (Mauchline 1998), and for this reason, they are very important to local fisheries (Wishner et al. 1988). They are herbivorous and can therefore exert top-down control on phytoplankton communities (Dagg and Turner 1982). They are cruise swimmers, and they often move in loops or spirals. Average swimming speed over a period of 60 minutes is 4.2 mm/s (1.3 BL/s) for upwards swimming and 13 mm/s (4 BL/s) for downwards swimming, where BL denotes body lengths (Mauchline 1998). *C. finmarchicus* has been shown to respond to mechanical cues corresponding to flow around an obstacle from a distance of $\sim$3 BL (Mauchline 1998). More recently, Woodson et al. (2007b) showed that this species increased swimming speed and turning frequency (behaviors indicative or area-restricted foraging behavior) when

Figure 2.5: Photographic image of*Calanus finmarchicus*, (photo from Mayor 2009)

exposed to a fluid mechanical cue (strain rate) consistent with that of a thin layer. The time spent in the layer (proportional residence time, PRT) also increased.

This change in behavior in *C. finmarchicus* is thought to be due to a cue hierarchy in which velocity gradients initially narrow search regions and chemical cues and food presence cause changes in behavior. This cue hierachy is an adaptation which allows copepods to spend their energy in areas that are likely to have food and mates in close proximity (Woodson et al. 2007a)

CHAPTER III

METHODS

In order to investigate the mechanosensing abilities of alpine copepod *Hesperodiaptomus shoshone*, male and females of this species were exposed separately to a horizontal shear layer. This flow was achieved via a laminar, planar free jet (the Bickley jet). The observation window ($10\ cm \times 10\ cm$) began 5 cm downstream of the jet origin and was illuminated with infra-red light during video capture. Free-swimming male or female copepods were recorded in both control (stagnant) and laminar shear layer conditions. These trajectories were then digitized and analyzed to correlate changes in behavior (swimming kinematics or gross trajectory characteristics) with local hydrodynamic cues.

3.1 Data Acquisition

3.1.1 Copepod Collection

H. shoshone were collected in August 2014 from Rock Pond (an alpine, glacier fed pond like the one shown in Figure 3.1) in the Shoshone National Forest in WY, USA, at an elevation of 10,789 feet. As described in Pender-Healy (2014), the copepods were collected by hand-retrieving a weighted $1/2\ m$ 33 μm-mesh plankton net thrown 6 m from the shore. For shipping, the copepods were transferred to thermoses filled with lake water at densities of 50 $copepods/L$ and insulated with ice packs. They were shipped overnight to Georgia Institute of Technology in Atlanta, GA. The animals were allowed to acclimate slowly to the ambient temperature of their home lake ($\sim 12°C$). They were then transferred in groups of 100 - 150 to 20-L containers filled with 15-L of artificial lake water (EPA medium) with the pH adjusted to match that of their home lakes (~ 8). The animals were fed daily with a mixture of lab hatched

Figure 3.1: An alpine pond fed by West Grasshopper Glacier on Mount Rearguard, of the Beartooth Mountains (Lyman 2012)

Artemia sp. and cultured *Daphnia spp.* The experiments were conducted over a 2 week period.

3.1.2 Experimental Design

The experimental design was very similar to that of True (2014), with the exception that the species used in this study is different. A laminar, planar free jet (the Bickley jet) was used in a recirculating flume system to mimic the fine-scale hydrodynamic structure of a horizontal shear layer. The flume measures 1 $m \times 25$ $cm \times 30$ cm and is made of clear acrylic (1.905 cm thick), allowing for video observation of two-dimensional free-swimming copepod trajectories. At the opposite end of the tank, a custom baffle was used to stabilize the free shear flow. The jet nozzle was designed to further stabilize the jet and ensure a uniform, top-hat velocity profile at the nozzle exit. A 12:1 ratio and 5^{th}-order polynomial contraction ensured that flow separation was prevented and turbulent fluctuations were minimized. Flow conditions screens, made of stainless steel mesh (50% open area), and a layer of high porosity

polypropylene sponge were added to further reduce turbulent fluctuations, as well as to distribute fluid momentum evenly across the width of the nozzle (Bickley 1937, Mehta and Bradshaw 1979, Hussein 1990, Woodson et al. 2005, True 2014).

The experimental setup is shown in Figure 3.2. The flow begins at the bottom reservoir (28 L, US Plastics), shown at the bottom right, which is filled with artificial lake water (EPA medium). The water flows through a 4 diaphragm, positive displacement pump (JABSCO Model 81701-1305) up to the constant head reservoir (28 L, US Plastics). The constant head reservoir is allowed to fill until it reaches the overflow level, at which point the water drains back into the bottom reservoir and begins to recirculate back to the constant head reservoir. The flow meter is then opened so that water flows through the inflow line into the planar jet nozzle (216 SS, jet opening 1 $cm \times 25$ cm) to create a laminar, planar jet in the test section. The jet flows through a flow-straightening baffle in order to prevent recirculation, flow instability, and exit geometry effects. The water then drains out of the main tank through the outflow line and back into the bottom reservoir.

During all *H. shoshone* behavioral assays, the jet operated at a volumetric flowrate of 16.8 cm^3/s (16 gph), which results in a maximum jet velocity, U_j of 6.7 mm/s and a jet Reynolds number ($Re_j = U_j d/\nu$) of ~ 50 (within the transitionally stable, laminar flow regime). This flowrate was selected in order to produce an ecologically-relevant laminar flowfield, meaning that the velocity and strain rate profiles and magnitudes in the test section were similar to those observed in thin layers of velocity gradients in the field. The velocity and strain rate magnitudes were also consistent with previous observations of behavior response among marine copepods (Woodson et al. 2005, Woodson et al. 2007a, Woodson et al. 2007b, True 2014).

All experiments were conducted in an environmental room at conditions as close as possible to those in-situ (water composition as well as temperature, 12°C). A total of eight trials were run: two male treatments (planar jet), two male controls (stagnant

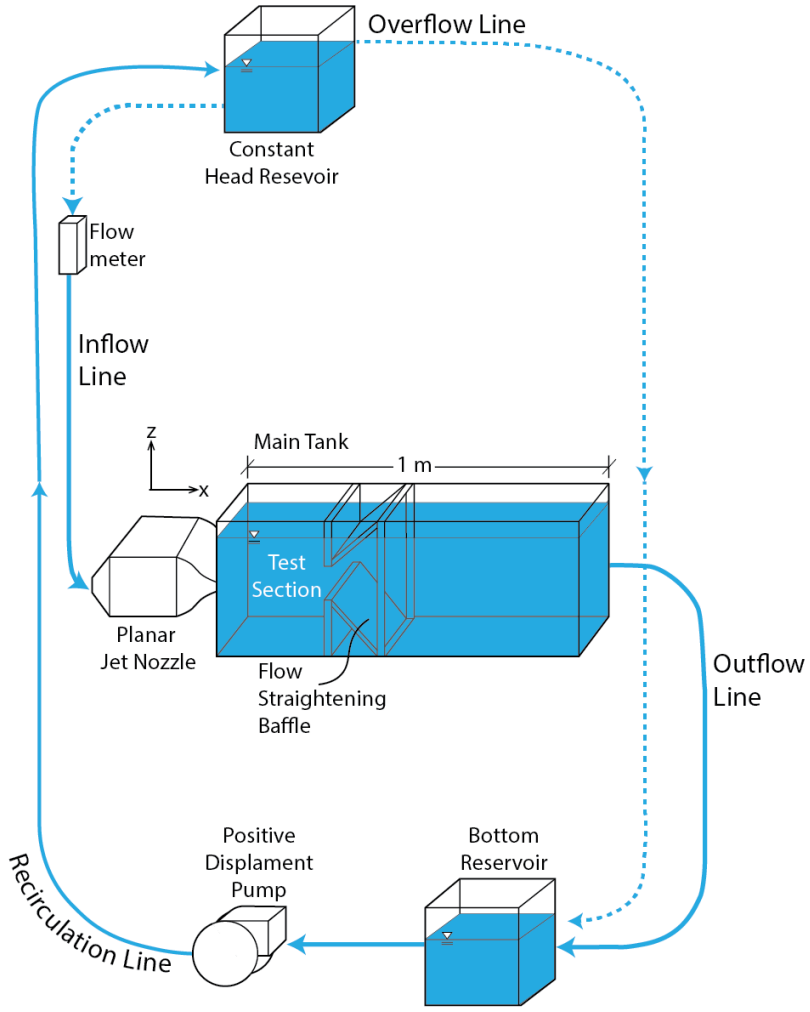

Figure 3.2: Experimental setup for *H. shoshone* behavioral assays, figure adapted from True (2014)

water), two female treatments, and two female controls. During each experiment, a group of 40 single-sex adult copepods were added to the trap in the upper left corner of the main tank, where they were held until recording began. The 10 $cm \times 10$ cm observation region, set 5 cm away from the jet origin and centered at the jet centerline, was illuminated by two IR diodies (CVI Melles Griot, 57 PNL 054/P4/S, >660 nm, 22 mW), which were diffused via 50° circular, top hat diffusers (Thor Labs model ED1-C50-MD). Infrared light was used for illumination because copepods have been

shown to react to light in at higher frequencies (Enright and Hamner 1967). Images were captured via a CCD video camera (Pulnix, 745i, 768 $\times$ 494 pixels), which was equipped with a 50 mm lens (Nikon AF Micro Nikkor) and linked to a digital video recorder (Sony, mini dv tapes). All experiments were recorded at 15 frames per second (fps).

3.2 Data Analyses

3.2.1 Threshold Shear Strain Rate and Kinematic Analyses

The mini dv tapes containing raw data were digitzed via iMovie HD (Apple Inc.) as a series of uncompressed avi (Audio-Video Interleave) clips, also at 15 fps. The animal trajectories were extracted using DLTdv5, a MATLAB-based digitization software (Hedrick 2008). Camera resolution was high enough - and the copepod large enough - that both head and tail positions could be obtained from the raw images. The centroid was interpolated as the midpoint between the head and tail points. The body length was calculated as the distance between the head and tail points ($d = \sqrt{(x_{head} - x_{tail})^2 - ((y_{head} - y_{tail})^2)}$) at each time step and then averaged over the entire observation time to get a single, representative body length for each animal. The trajectories (x_{head}, z_{head}; x_{tail}, z_{tail}; $x_{centroid}$, $z_{centroid}$; t) were then analyzed via custom MATLAB codes.

The following procedure was adapted from True (2014). First, the path kinematics such as relative swimming speed and body orientation (or angle) were computed for the entirety of each trajectory. Then the centerline jet velocity was used to determine the shear strain rate value at the head location (x_{head}, z_{head}) at each time point in each trajectory. For each trajectory, the mean and standard deviation of each path kinematic parameter was calculated above and below a certain shear strain rate threshold. This threshold was varied in accordance with the values observed in the Bickley jet ($0.001 - 0.3s^{-1}$). The absolute difference in these values - above

and below the threshold - is computed for every threshold value and then normalized by the maximum difference. The resulting data set is called the behavior response curve (True et al. 2015). The behavior response curve is calculated for every trajectory, and then all 40 response curves are ensemble averaged for each shear strain rate value. This entire procedure was done for the following path kinematics parameters: relative swimming speed (BL/s); acceleration (BL/s^2); relative head to tail speed, RHT ($|v_{head} - v_{tail}|$); rotation translation spectrum, RTS ($|\frac{v_{head}-v_{tail}}{max(v_{head},v_{tail})}|$); body orientation (or angle), BA; and heading change, HC (the change in body orientation, $BA_{t+1} - BA_t$). Once normalized, these ensemble-averaged behavior response curves can be averaged across parameters once again for each strain rate to yield a single behavior response curve for each trial (male or female treatment). By plotting this final behavior response curve, the actual threshold shear strain rate can be identified from the graph as the point that corresponds to a rapid change in the slope of the curve.

Once the threshold shear strain rate value was determined using the procedure above, that threshold value is denoted as the edge of what will here after be referred to as the "layer," meaning the region of shear that the animal appears to sense which need not be the entire shear region created by the jet. The shear strain rate threshold is used to divide the observation window into two distinct geometric regions: in-layer, in which most shear strain rate values are greater than the threshold, and out-of-layer, in which all shear strain rate values are less than the threshold. Once these geometric regions are determined, statistical comparisons can be made for individual animal trajectories based both on location (in-layer vs. out-of-layer) as well as exposure (pre-contact vs. post-contact).

Of all the kinematics parameters calculated, only relative swimming speed (mm/s and BL/s) and turn frequency (TF) were examined in the statistical analysis to follow. A turn is defined as a change of 15° or more in heading direction over a period

of 0.33 s (5 data points at 15 fps). The frequency of turns then is the number of turns divided by the time of observation. The gross parameters calculated were net-to-gross displacement ratio ($NGDR$ = net displacement/gross displacement); proportional residence time (PRT =time spent in-layer/total time in observation window); and proportional vicinity time (PVT = time spent after contact with the layer/total time in observation window).

Histograms were made of body orientation, and the mean angle and angular deviation were found according to the procedure outlined for circular distributions in Zar (1999). The body vector was defined from tail to head ($x_{head} - x_{tail}$,$z_{head} - z_{tail}$). The 0° direction corresponds to the direction of flow and 180° corresponds to the direction against flow.

3.2.2 Statistical Analyses

Statistical analyses of the behavior responses (kinematic and gross parameters) was conducted using JMP Pro 11 (2013, SAS Institute). Significance of changes in relative swimming speed (BL/s and mm/s) and TF were analyzed using a three-factor, nested, repeated measures, ANOVA, for pre-contact vs. post-contact (exposure) values as well as in-layer vs. out-of-layer (location) values. The three factors used were treatment, sex, and location (or exposure). The repeated measures aspect means that values were compared for each individual animal. The nested aspect of the design means that variability was allowed across replicates, but if replicate effects were found to be insignificant, the replicates were pooled. Significance of changes in gross parameters (NGDR, PRT, PVT) were evaluated using a two-factor (treatment and sex), nested ANOVA of the arcsine transformed data sets for control vs. treatment and male vs. female.

CHAPTER IV

RESULTS AND DISCUSSION

4.1 Results

4.1.1 Shear Strain Rate Threshold

An example of a digitized trajectory is shown in Figure 4.1. The head and tail points were tracked directly, and the centroid was interpolated as the midpoint between each head and tail point. More example trajectories of the centroid location are shown for each experiment in Figures 4.2 and 4.3.

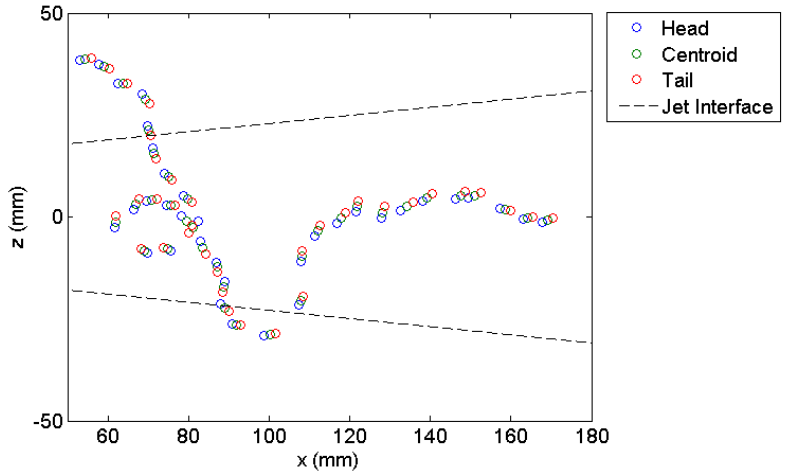

Figure 4.1: Sample head, centroid, and tail points of a single copepod track (species: *Hesperodiaptomus shoshone*). Every twelfth data point is shown for clarity's sake. The layer edge, based on a shear strain rate threshold of $0.1s^{-1}$, yielded from the shear strain rate threshold analysis, is marked by the dashed line.

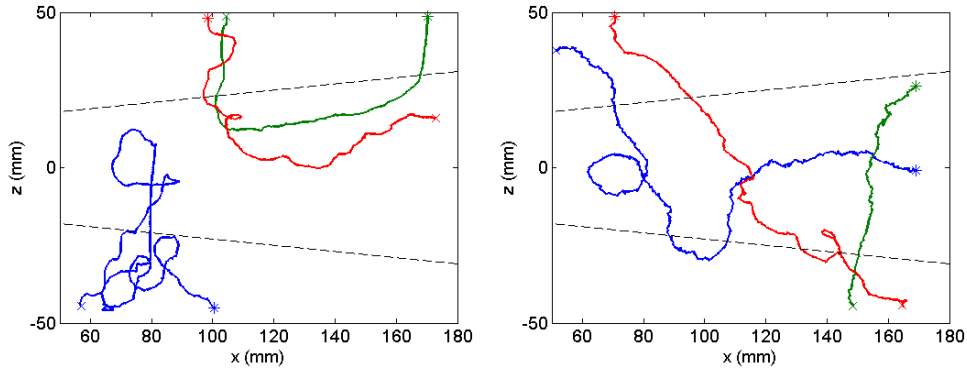

(a) Male treatment, replicate 1

(b) Male treatment, replicate 2

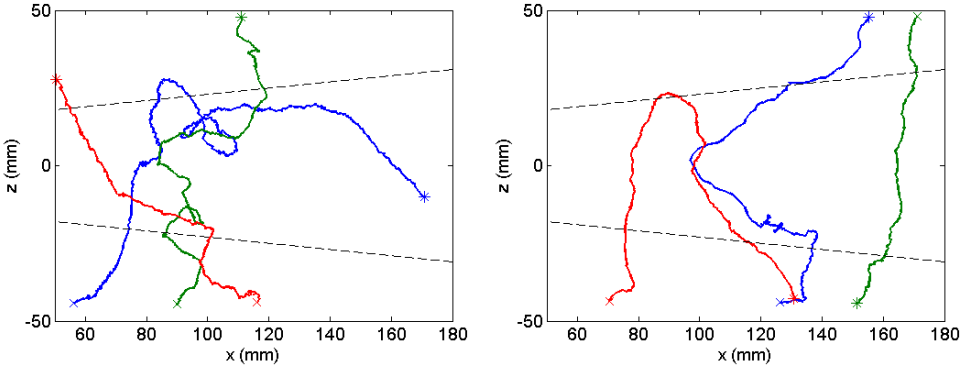

(c) Male control, replicate 1

(d) Male control, replicate 2

Figure 4.2: Sample trajectories for the male *Hesperodiaptomus shoshone* experiments. Only centroid locations are shown. The layer edge, based on a shear strain rate threshold of $0.1s^{-1}$, yielded from the shear strain rate threshold analysis, is marked by the dashed line. Each beginning point is indicated with an asterisk and each ending point with an 'x'

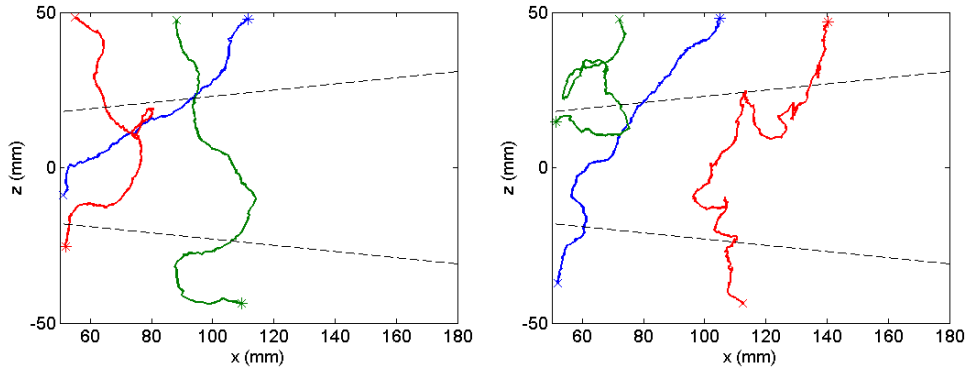

(a) Female treatment, replicate 1

(b) Female treatment, replicate 2

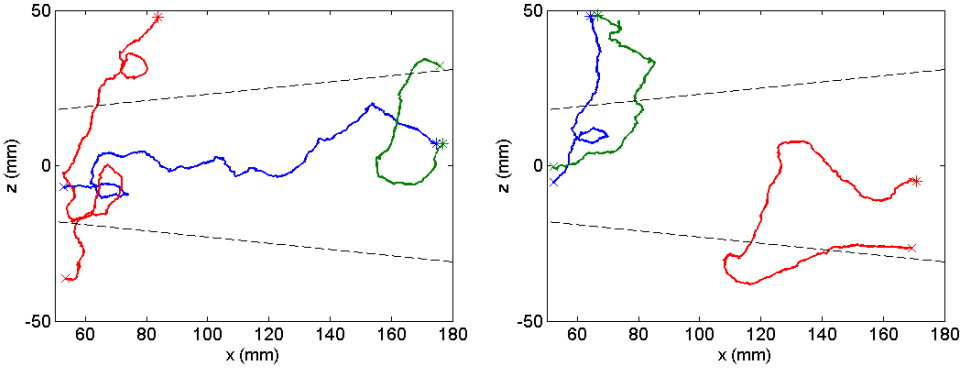

(c) Female control, replicate 1

(d) Female control, replicate 2

Figure 4.3: Sample trajectories for the female *Hesperodiaptomus shoshone* experiments. Only centroid locations are shown. The layer edge, based on a shear strain rate threshold of $0.1s^{-1}$, yielded from the shear strain rate threshold analysis, is marked by the dashed line. Each beginning point is indicated with an asterisk and each ending point with an 'x'

The first step is to determine a behavior threshold that defines the strain rate value at which the copepods appear to respond to the velocity gradient. The behavior threshold will be used to define the boundaries of the shear layer treatment region. The behavior response curves are created by examining a particular behavior parameter for a single trajectory at different shear strain rate values encountered along the

trajectory. For each trajectory, at every shear strain rate value encountered, the absolute difference of both the mean and standard deviation of the behavior parameter above and below that shear strain rate value is calculated. Each data point is normalized by the maximum difference. This procedure is repeated for each trajectory, which maintains individual variation. The data points are then ensemble averaged over each shear strain rate value to yield the population level trends.

Male behavior response curves are shown in Figure 4.4. In Figures 4.4a and 4.4b, the normalized change for each behavior parameter (speed, acceleration, RHT, RTS, BA, and HC) is plotted against the strain rate value. These multiple curves are ensemble averaged to produce the normalized change in mean and standard deviation across all behavior parameters, producing the total behavior response curves shown in Figure 4.4c. A similar set of curves is shown in Figure 4.5 for the female set of experiments.

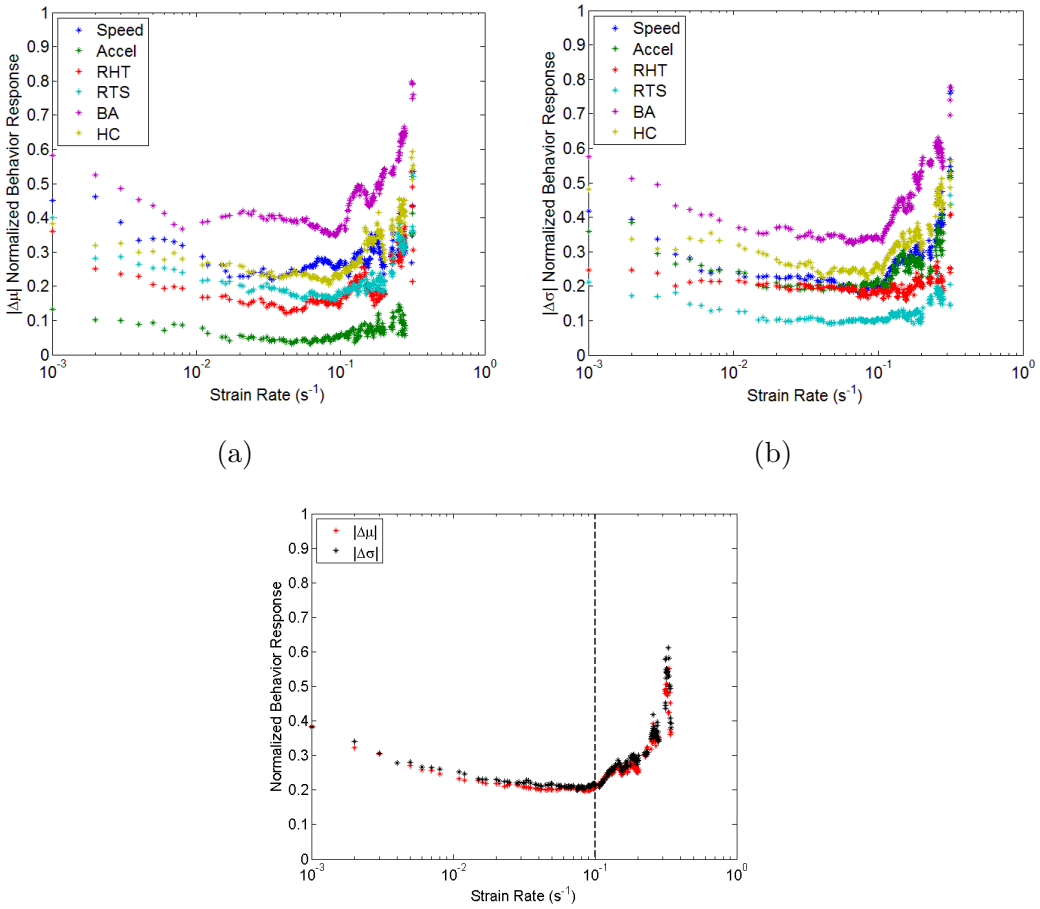

Figure 4.4: *Hesperodiaptomus shoshone* male behavior response curves (2.37 ± 0.29 *mm*). (a) the normalized change in the mean of a behavior parameter plotted against shear strain rate value (i.e., difference in the mean value calculated above and below the strain rate value), (b) the normalized change in the standard deviation of a behavior parameter, and (c) all the behavior parameters are ensemble-averaged to produce the total behavior response curve.

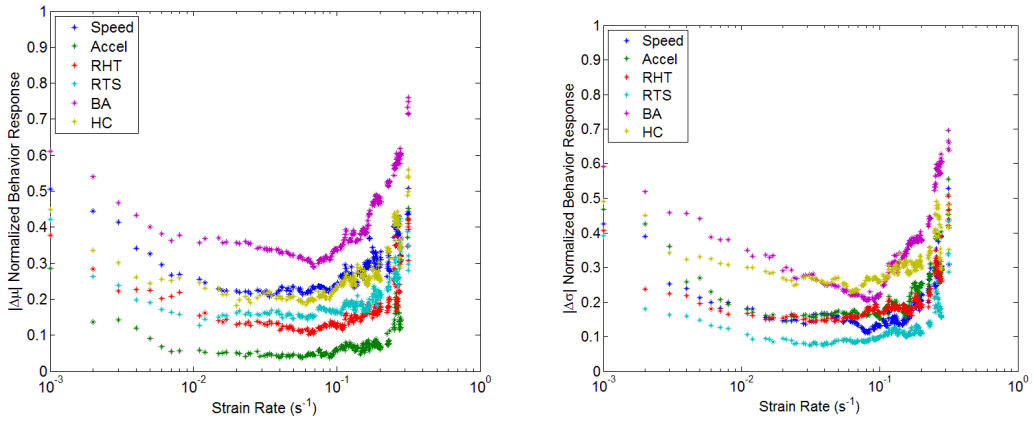

(a)

(b)

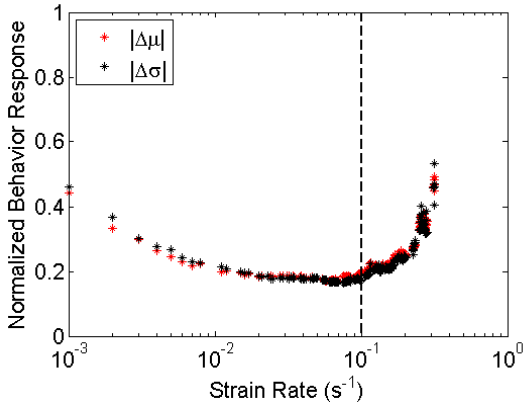

(c)

Figure 4.5: *Hesperodiaptomus shoshone* female behavior response curves (2.54 ± 0.37 *mm*). (a) the normalized change in the mean of a behavior parameter plotted against shear strain rate value (i.e., difference in the mean value calculated above and below the strain rate value), (b) the normalized change in the standard deviation of a behavior parameter, and (c) all the behavior parameters are ensemble-averaged to produce the total behavior response curve.

The threshold is determined by identifying the shear strain rate value at which the slope of the behavior response curve changes rapidly. This location of rapid change denotes the location where the difference in the mean and standard deviation above and below that shear strain rate value changes, therefore denoting a threshold at

which the copepod behavior changes. Both the male and female behavior response curves appear to have a transition in slope at a shear strain rate threshold of 0.1 s^{-1} (highlighted via a vertical dashed line in Figures 4.4c and 4.5c), hence this value is selected as the behavior threshold.

4.1.2 Kinematics and Gross Parameters

The shear strain rate threshold is used to divide the observation window into two distinct geometric regions: in-layer, in which most shear strain rate values are greater than the threshold, and out-of-layer, in which all shear strain rate values are less than the threshold. Once these geometric regions are determined, statistical comparisons can be made for individual animal trajectories based both on location (in-layer vs. out-of-layer) as well as exposure (pre-contact vs. post-contact). The same geometric region can be defined for the control cases to find portions of the trajectories that are in-layer and out-of-layer as well as pre-contact and post-contact, just as in the treatment cases.

In Figures 4.6 and 4.7, relative swimming speed (mm/s) in-layer vs. out-of layer and pre-contact vs. post-contact, respectively, are shown for the treatment (shear layer) and control. These data are summarized in Tables 4.1 and 4.3, respectively. The mean values, as well as standard error values, are shown for each sex and for each experiment (control or treatment). The results of the repeated-measures ANOVA are given in Tables 4.2 and 4.4, respectively.

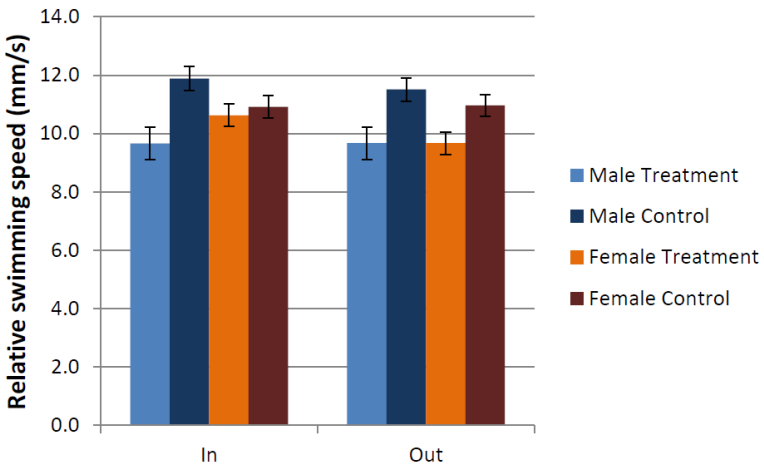

Figure 4.6: Relative swimming speed (mm/s) in-layer and out-of-layer, defined by a shear strain rate threshold of 0.1 s^{-1}. The error bars are ± 1 SE.

Table 4.1: Relative swimming speed (mm/s) in-layer and out-of-layer [mean (SE)]. The layer is defined by a shear strain rate threshold of 0.1 s^{-1}.

Sex	Experiment	n	In-layer	Out-of-layer
Male	Control	80	11.87 (0.41)	11.49 (0.38)
	Treatment	80	9.66 (0.53)	9.67 (0.56)
Female	Control	80	10.91 (0.35)	10.96 (0.38)
	Treatment	80	10.63 (0.28)	10.60 (0.26)

Table 4.2: The results for the three-factor, repeated measures ANOVA for relative swimming speed (mm/s) in-layer vs. out-of-layer (location). Treatment, sex, and location effects are shown, as well as the interaction between and among these effects. Significant results correspond to a $p \leq 0.05$ and are denoted by an asterisk (*).

Source of Variability	**Mean Squares**	**Degrees of Freedom (df)**	**F**	**p**
Treatment	0.034	1	10.45	0.0014*
Sex	9×10^{-5}	1	0.027	0.870
Location	4×10^{-4}	1	0.126	0.723
Sex × Treatment	0.017	1	5.40	0.021*
Sex × Location	6×10^{-4}	1	0.200	0.657
Treatment × Location	0.001	1	0.361	0.549
Sex × Treatment × Location	0.002	1	0.643	0.432
Within Subjects	0.004	3	0.126	0.754

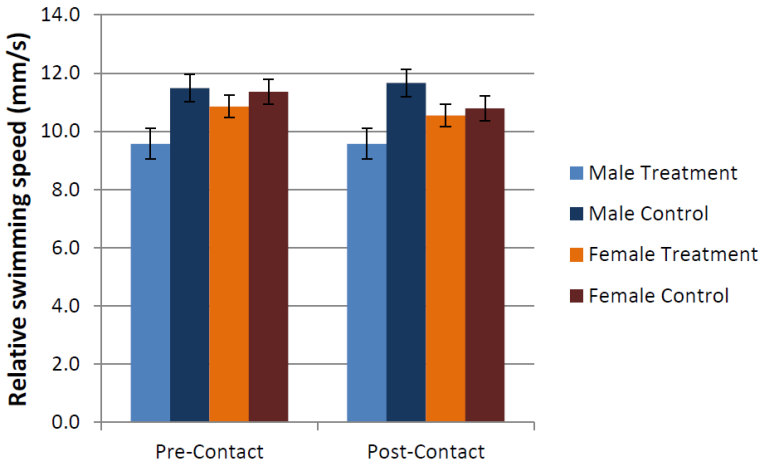

Figure 4.7: Relative swimming speed (mm/s) pre-contact and post-contact, defined by a shear strain rate threshold of 0.1 s^{-1}. The error bars are ± 1 SE.

Table 4.3: Relative swimming speed (mm/s) pre-contact and post-contact [mean (SE)]. The layer is defined by a shear strain rate threshold of 0.1 s^{-1}.

Sex	Experiment	n	Pre-contact	Post-contact
Male	Control	80	11.48 (0.47)	11.66 (0.39)
	Treatment	80	9.56 (0.53)	9.56 (0.42)
Female	Control	80	11.36 (0.42)	10.78 (0.36)
	Treatment	80	10.85 (0.39)	10.54 (0.26)

Table 4.4: The results for the three-factor, repeated measures ANOVA for relative swimming (mm/s) pre-contact vs. post-contact (exposure). Treatment, sex, and exposure effects were analyzed, as well as the interaction between and among these effects. Significant results correspond to a p-value of $p \leq 0.05$ and are denoted by an asterisk (*).

Source of Variability	**Mean Squares**	**Degrees of Freedom (df)**	**F**	**p**
Treatment	0.036	1	9.13	0.003*
Sex	3×10^{-4}	1	0.46	0.50
Exposure	0.003	1	0.79	0.37
Sex × Treatment	0.001	1	2.77	0.096
Sex × Exposure	0.008	1	2.06	0.15
Treatment × Exposure	2×10^{-4}	1	0.05	0.82
Sex × Treatment × Exposure	2×10^{-6}	1	0.0005	0.98
Within Subjects	0.009	3	0.713	0.55

For relative swimming speed (mm/s), the treatment effect is significant, but neither the location nor the exposure effects is significant. Moreover, the treatment effect

is not contingent on the copepod's location or its exposure to the layer. In general, the copepods swim more slowly in treatment than control. However, the significant changes in behavior due to the treatment does have some dependence on the sex of the animal in the case of the in-layer vs. out-of-layer analyses, whereas there is no such dependence for the pre-contact vs. post-contact analyses. The decrease in swimming speed for males from control to treatment is more drastic than that of females. In Figure 4.8, the male and female results were pooled to show the differences between treatment and control directly.

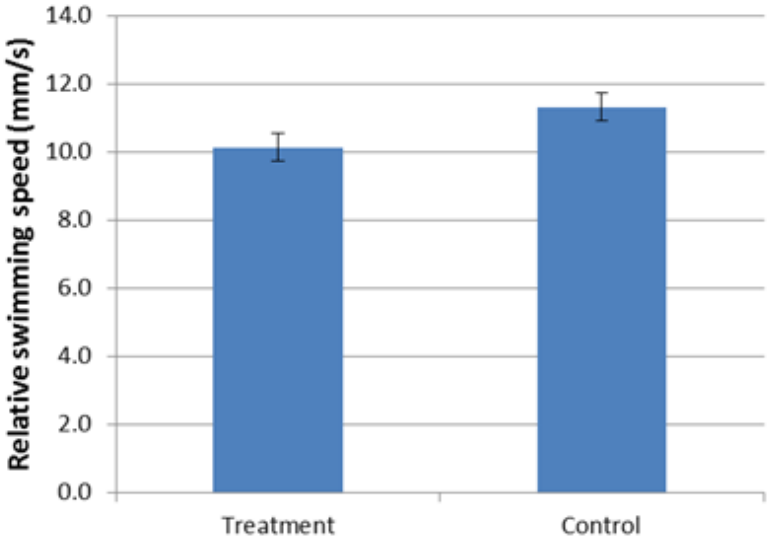

Figure 4.8: Relative swimming speed (mm/s) with male and female data pooled to show the differences between treatment and control directly. The error bars are $\pm 1SE$.

The swimming speed for each animal can be non-dimensionalized in terms of body lengths. Body length of each copepod was determined based on the head and tail locations obtained for the individual tracks. These data, both in-layer vs. out-of-layer and pre-contact vs. post-contact, are shown in Figures 4.9 and 4.10, respectively. These data are summarized in Tables 4.5 and 4.7, respectively. The results of the repeated-measures ANOVA are given in Tables 4.6 and 4.8, respectively.

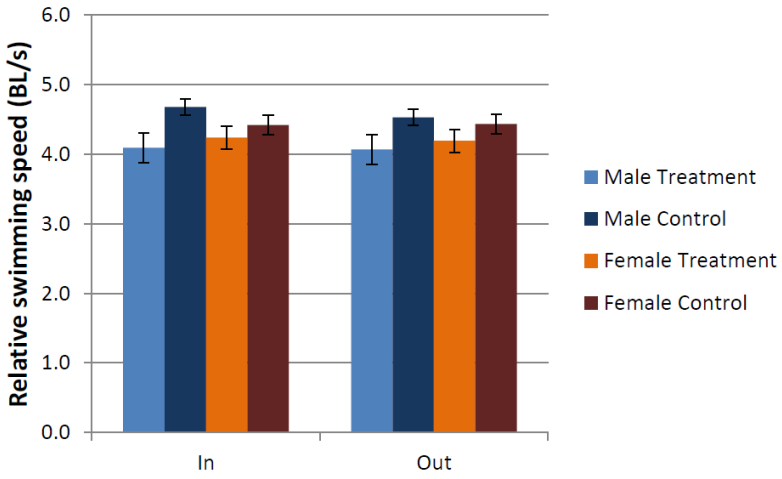

Figure 4.9: Relative swimming speed (BL/s) in-layer and out-of-layer, defined by a shear strain rate threshold of 0.1 s^{-1}. The error bars are ± 1 SE.

Table 4.5: Relative swimming speed (BL/s) in-layer and out-of-layer [mean (SE)].

Sex	Experiment	n	In-layer	Out-of-layer
Male	Control	80	4.68 (0.16)	4.53 (0.15)
	Treatment	80	4.09 (0.18)	4.07(0.22)
Female	Control	80	4.42 (0.13)	4.44 (0.14)
	Treatment	80	4.24 (0.12)	4.19 (0.09)

Table 4.6: The results for the three-factor, repeated measures ANOVA for relative swimming speed (BL/s) in-layer vs. out-of-layer (location). Treatment, sex, and location effects are shown, as well as the interaction between and among these effects. Significant results correspond to a $p \leq 0.05$ and are denoted by an asterisk (*).

Source of Variability	**Mean Squares**	**Degrees of Freedom (df)**	**F**	**p**
Treatment	0.022	1	6.84	0.009*
Sex	2×10^{-4}	1	0.068	0.79
Location	0.001	1	0.330	0.56
Sex × Treatment	0.003	1	1.05	0.31
Sex × Location	7×10^{-4}	1	0.214	0.46
Treatment × Location	5×10^{-4}	1	0.160	0.69
Sex × Treatment × Location	0.002	1	0.560	0.46
Within Subjects	0.003	3	0.311	0.82

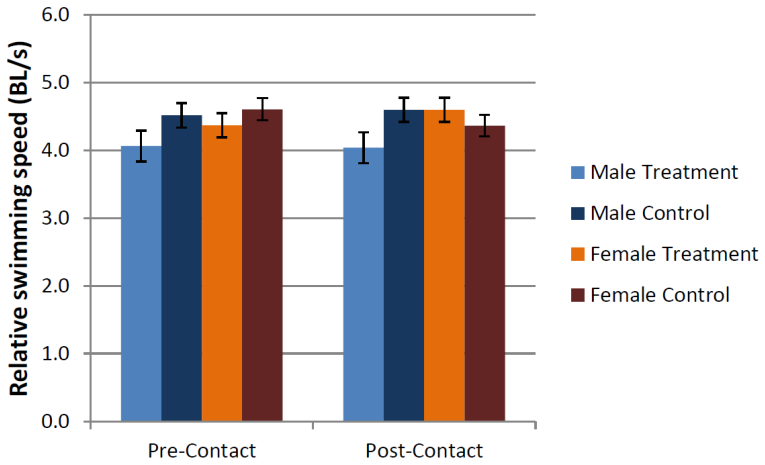

Figure 4.10: Relative swimming speed (BL/s) pre-contact and post-contact, defined by a shear strain rate threshold of 0.1 s^{-1}. The error bars are ± 1 SE.

Table 4.7: Relative swimming speed (BL/s) pre-contact and post-contact [mean (SE)].

Sex	Experiment	n	Pre-contact	Post-contact
Male	Control	80	4.52 (0.18)	4.60 (0.16)
	Treatment	80	4.06 (0.23)	4.04 (0.17)
Female	Control	80	4.61 (0.16)	4.36 (0.13)
	Treatment	80	4.37 (0.18)	4.18 (0.10)

Table 4.8: The results for the three-factor, repeated measures ANOVA for relative swimming (BL/s) pre-contact vs. post-contact (exposure). Treatment, sex, and exposure effects were analyzed, as well as the interaction between and among these effects. Significant results correspond to a p-value of $p \leq 0.05$ and are denoted by an asterisk (*).

Source of Variability	**Mean Squares**	**Degrees of Freedom (df)**	**F**	**p**
Treatment	0.020	1	5.09	0.025*
Sex	7×10^{-4}	1	0.19	0.67
Exposure	0.004	1	1.02	0.31
Sex × Treatment	0.002	1	0.348	0.56
Sex × Exposure	0.009	1	2.21	0.14
Treatment × Exposure	4×10^{-4}	1	0.093	0.76
Sex × Treatment × Exposure	4×10^{-6}	1	0.001	0.98
Within Subjects	0.009	3	0.777	0.51

When non-dimensionalized, the interaction of the treatment effect and sex is no longer significant, leaving only a significant treatment effect. This means that there

is a signficiant difference between and control and treatment, but that the difference is not dependent on whether the animal is a male or a female. Once again, there is no effect due to location or exposure, and there is no interaction between the treatment effect and these parameters. In Figure 4.11, the male and female results were pooled to show the differences between treatment and control directly.

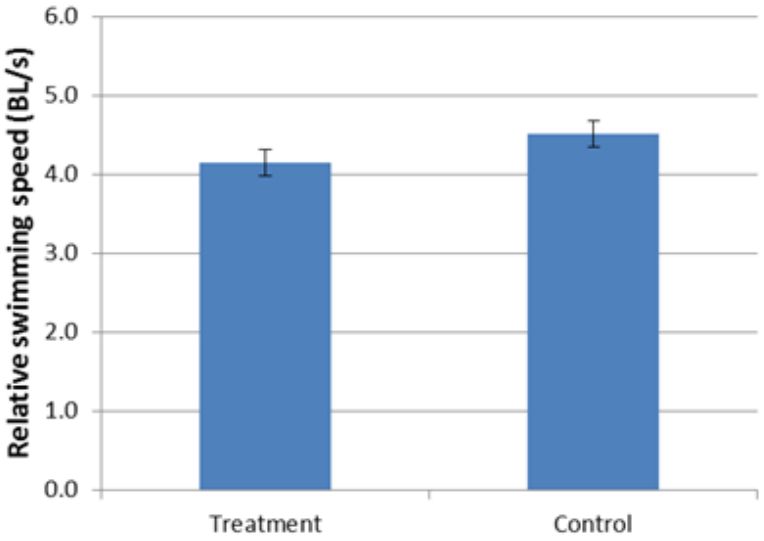

Figure 4.11: Relative swimming speed (BL/s) with male and female data pooled to show the differences between treatment and control directly. The error bars are $\pm 1SE$.

Turn frequency both in-layer vs. out-of-layer and pre-contact vs. post-contact are shown in Figures 4.12 and 4.13, respectively. These data are summarized in Tables 4.9 and 4.11, respectively. The ANOVA statistics are shown in Tables 4.10 and 4.12, respectively. Here, a turn is defined as a change of greater than 15° over a period of 0.33 seconds (or 5 time points of data).

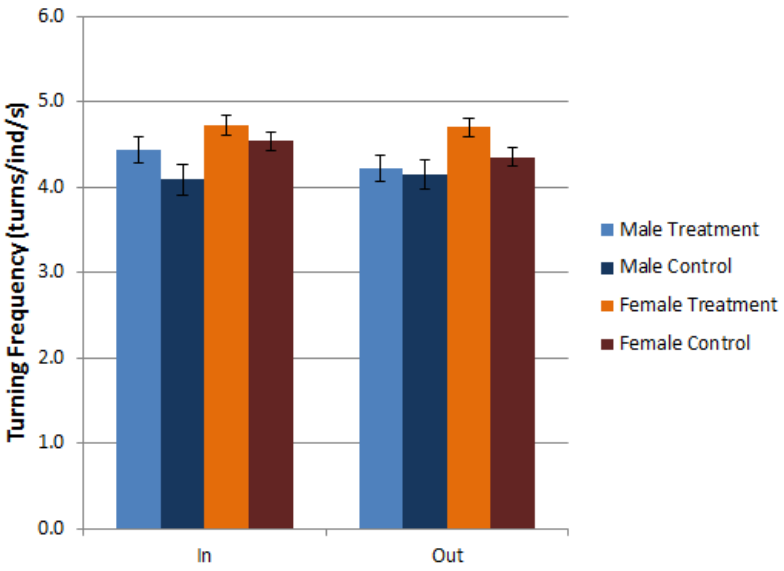

Figure 4.12: Turn frequency ($turns/ind/s$) in-layer and out-of-layer, defined by a shear strain rate threshold of 0.1 s^{-1}. The error bars are ± 1 SE.

Table 4.9: Turn frequency ($turns/ind/s$) in-layer and out-of-layer [mean (SE)].

Sex	Experiment	n	In-layer	Out-of-layer
Male	Control	80	4.09 (0.16)	4.13 (0.14)
	Treatment	80	4.43 (0.15)	4.19 (0.12)
Female	Control	80	4.54 (0.11)	4.35 (0.11)
	Treatment	80	4.72 (0.12)	4.70 (0.11)

Table 4.10: The results for the three-factor, repeated measures ANOVA for turning frequency ($turns/ind/s$) in-layer vs. out-of-layer (location). Treatment, sex, and location effects are shown, as well as the interaction between and among these effects. Significant results correspond to a $p \leq 0.05$ and are denoted by an asterisk (*).

Source of Variability	**Mean Squares**	**Degrees of Freedom (df)**	**F**	**p**
Treatment	0.01	1	3.17	0.076
Sex	0.075	1	22.2	< 0.0001*
Location	0.003	1	0.96	0.33
Sex $\times$ Treatment	0.085	1	0.96	$<$0.0001*
Sex $\times$ Location	2×10^{-5}	1	26.3	0.81
Treatment $\times$ Location	2×10^{-4}	1	0.059	0.82
Sex $\times$ Treatment $\times$ Location	2×10^{-4}	1	0.053	0.81
Within Subjects	4×10^{-4}	3	0.040	0.99

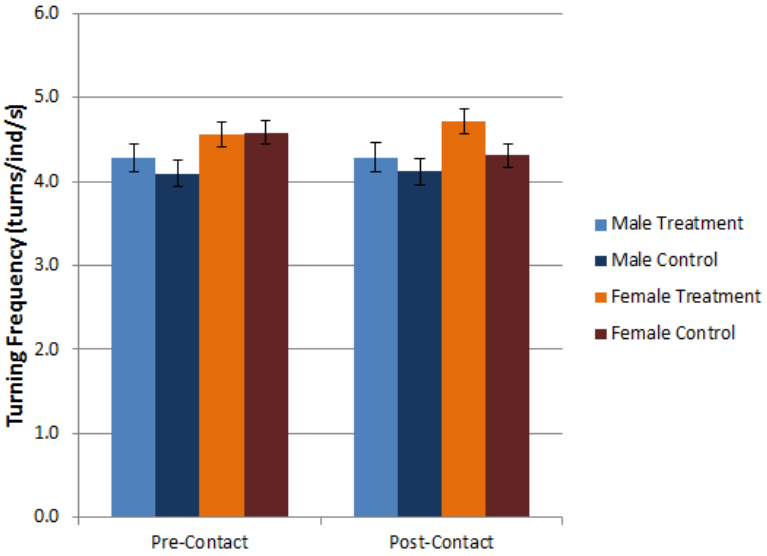

Figure 4.13: Turn frequency ($turns/ind/s$) pre-contact and post-contact, defined by a shear strain rate threshold of 0.1 s^{-1}. The error bars are $\pm 1SE$.

Table 4.11: Turn frequency ($turns/ind/s$) pre-contact and post-contact [mean (SE)].

Sex	Experiment	n	Pre-contact	Post-contact
Male	Control	80	4.10 (0.17)	4.07 (0.13)
	Treatment	80	4.28 (0.17)	4.25 (0.13)
Female	Control	80	4.56 (0.14)	4.27 (0.10)
	Treatment	80	4.55 (0.15)	4.79 (0.10)

Table 4.12: The results for the three-factor, repeated measures ANOVA for turning frequency ($turns/ind/s$) pre-contact vs. post-contact (exposure). Treatment, sex, and exposure effects were analyzed, as well as the interaction between and among these effects. Significant results correspond to a p-value of $p \leq 0.05$ and are denoted by an asterisk (*).

Source of Variability	**Mean Squares**	**Degrees of Freedom (df)**	**F**	**p**
Treatment	0.017	1	4.23	0.041*
Sex	0.097	1	24.5	<0.0001*
Exposure	0.006	1	1.42	0.23
Sex × Treatment	0.05	1	12.6	0.0005*
Sex × Exposure	0.003	1	0.681	0.41
Treatment × Exposure	0.009	1	2.29	0.13
Sex × Treatment × Exposure	0.012	1	2.98	0.086
Within Subjects	0.023	3	1.96	0.12

For turning frequency ($turns/ind/s$), there is a significant difference due the sex of the copepod for both the in-layer vs. out-of-layer and pre-contact vs. post-contact analyses. In general, females have higher turn frequencies than the males. For the pre-contact vs. post-contact analyses, there is also a treatment effect and an interaction effect between sex and treatment. Turn frequency increases between control and treatment for both sexes, excepting pre-contact for females. While the treatment effect in the in-layer vs. out of layer analyses is not significant, it is marginally significant with a p-value of 0.076. There is also an interaction effect between treatment and sex in the in-layer vs. out-of-layer analyses. Once again, none of these significant differences are dependent upon the animals location relative to the layer or their exposure to the layer, and there are no effects due to either of location or

exposure. In Figure 4.14, the treatment and control results were pooled to show the differences between males and females directly. Figure 4.15 shows the differences between treatment and control, with the sexes pooled together.

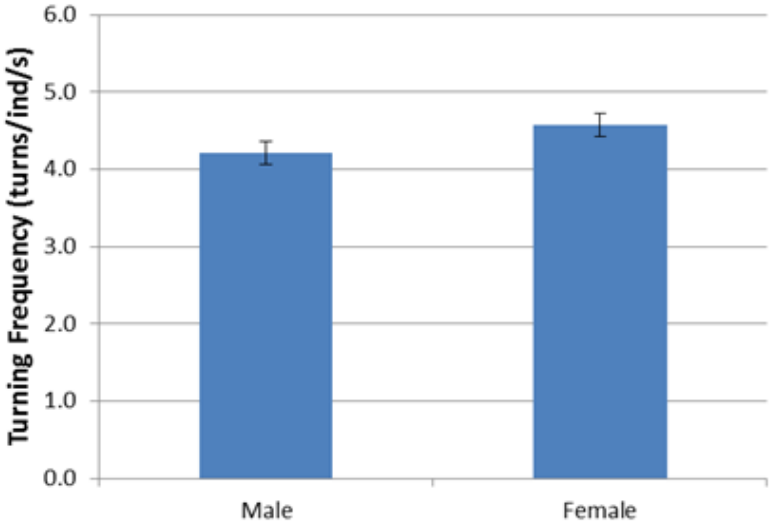

Figure 4.14: Turn frequency ($turns/ind/s$) with male and female data pooled to show the differences between sexes directly.. The error bars are $\pm 1SE$.

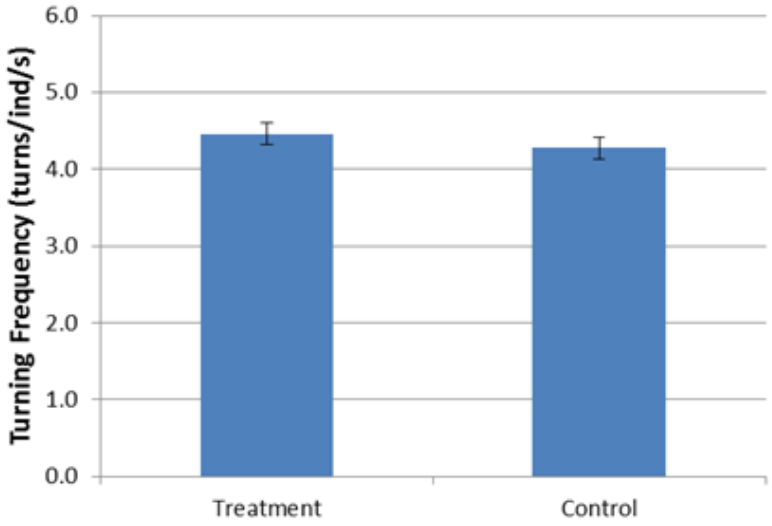

Figure 4.15: Turn frequency ($turns/ind/s$) with male and female data pooled to show the differences between treatment and control directly. The error bars are $\pm 1SE$.

Net-to-gross displacement ratio (NGDR) values for control and treatment are

shown in Figure 4.16. The data are summarized in Table 4.13. The ANOVA statistics are shown in Table 4.14. There is a significant sex effect, indicating that males move in significantly straighter lines than females, corresponding to higher values of NGDR. However, there is no significant effect of the treatment on NGDR.

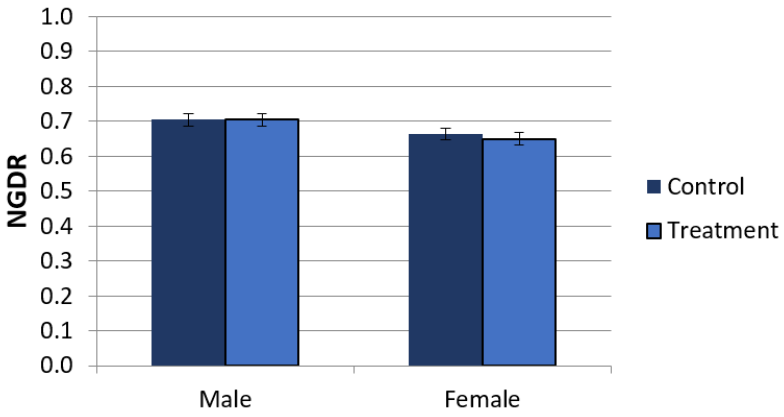

Figure 4.16: Net-to-gross-displacement ratio (NGDR) for treatment and control for both sexes. The error bars are ± 1 SE.

Table 4.13: Net-to-gross displacement ratio (NGDR) [mean (SE)].

Sex	Experiment	n	NGDR
Male	Control	80	0.72 (0.004)
	Treatment	80	0.72 (0.004)
Female	Control	80	0.67 (0.003)
	Treatment	80	0.66 (0.003)

Table 4.14: The results for the two-factor, repeated measures ANOVA for net-to-gross displacement ratio (NGDR). Treatment and sex effects are shown, as well as the interaction effects. Significant results correspond to a $p \leq 0.05$ and are denoted by an asterisk (*).

Source of Variability	**Mean Squares**	**Degrees of Freedom (df)**	**F**	**p**
Treatment	0.004	1	0.042	0.838
Sex	0.406	1	4.01	0.046*
Sex × Treatment	0.005	1	0.054	0.837

The proportional vicinity time (PVT) and proportional residence time (PRT) for control and shear are shown in Figure 4.17. The data are summarized in Table 4.15. The ANOVA statistics are shown in Tables 4.16 and 4.17, respectively. There was a significant treatment effect for PVT, which had no significant interaction; PVT was larger for treatment compared to control. There were no significant changes in PRT for either treatment or sex.

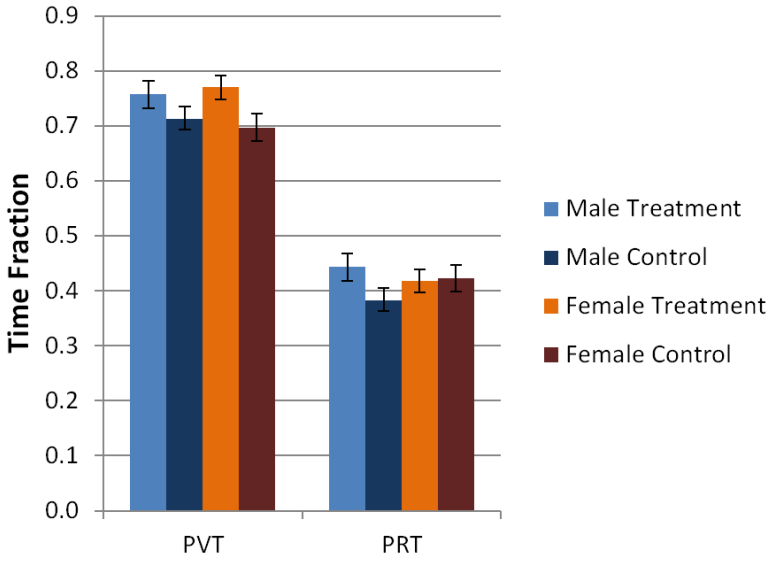

Figure 4.17: Proportional vicinity time (PVT) and proportional residence time (PRT) for treatment (shear) and control. The error bars are ± 1 SE.

Table 4.15: Proportional vicinity time (PVT) [mean (SE)] and proportional residence time (PRT) [mean (SE)].

Sex	Treatment	n	PVT	PRT
Male	Control	80	0.76 (0.001)	0.38 (0.008)
	Treatment	80	0.81 (0.001)	0.44 (0.008)
Female	Control	80	0.76 (0.001)	0.43 (0.007)
	Treatment	80	0.82 (0.001)	0.42 (0.007)

Table 4.16: The results for the two-factor, repeated measures ANOVA for proportional vicinity time (PVT). Treatment and sex effects are shown, as well as the interaction effects. Significant results correspond to a $p \leq 0.05$ and are denoted by an asterisk (*).

Source of Variability	**Mean Squares**	**Degrees of Freedom (df)**	**F**	**p**
Treatment	0.0006	1	8.62	0.004*
Sex	0.282	1	0.019	0.891
Sex × Treatment	0.017	1	0.526	0.469

Table 4.17: The results for the two-factor, repeated measures ANOVA for proportional residence time (PRT). Treatment and sex effects are shown, as well as the interaction effects. Significant results correspond to a $p \leq 0.05$ and are denoted by an asterisk (*).

Source of Variability	**Mean Squares**	**Degrees of Freedom (df)**	**F**	**p**
Treatment	0.005	1	0.085	0.771
Sex	0.065	1	1.17	0.28
Sex × Treatment	0.123	1	2.23	0.137

We performed an extensive analysis of body orientation angle. Visual inspection of the plots of the results indicated there were no observable preferences in body angle direction for in-layer vs. out-of-layer or pre-contact vs. post-contact, and therefore statistical analyses were not conducted. The mean of body angle was calculated for each experimental run. For display, the mean for each individual copepod is plotted on a polar diagram in the Appendix. The ensemble average of the mean

body angle data indicates the direction and strength of a preference for a particular orientation. The figures are provided in the Appendix. Histograms of body angle are also provided in the Appendix. The width of each wedge corresponds to the angle range, which was 18 deg, and the length of each bar represents the percentage of data that falls within that particular angle range. Again, the figures indicated there were no observable preferences in body angle orientation, and therefore statistical analyses were not conducted.

4.2 Discussion

Freshwater copepod *H. shoshone* consistently showed differences in kinematic parameters due to the presence of the thin layer shear flow treatment, excepting turning frequency ($turns/ind/s$) in the in-layer vs. out-of-layer analyses. The copepods significantly decreased their relative swimming speed (mm/s and $bodylengths/s$) from control to treatment in both the location and exposure analyses, which is consistent with a corresponding significant increase in the proportional vicinity time. If the animals are swimming more slowly, we would expect the time that they spend in the observation window to increase, which may cause an increase in PVT (as observed). The interaction effect between sex and treatment is not present in the non-dimensionalized swimming speed, indicating that interaction effect in the dimensional case is due merely due to body size differences between males (2.37 ± 0.29 mm) and females ($2.54 \pm 0.37mm$).

There was a also treatment effect in turning frequency in the exposure analysis, but this effect was only marginally significant in the location analyses ($p = 0.076$). In both analyses, the copepods increased their turning frequency from control to treatment. Significant differences between sexes were also observed in turning frequency, with females turning more than males. This result is consistent with a lower net-to-gross displacement ratio, which indicates curvier paths, for the females compared to the

males. The sex effect in turning frequency could be the reason that the treatment effect in the location analyses is not significant. Because the males have overall lower turning frequencies than the females, pooling these sets of data together adds more variability to the sample that could obscure significant effects. This is supported by the interaction effect between sex and treatment in both the location and exposure analyses.

Our data shows that *H. shoshone* exhibits a global response to the shear layer that is not localized to the layer region itself. However, none of these significant differences depended upon the animals' location within (or without) the layer or their exposure to the layer. In addition, there was no interaction between the treatment effect and the location or exposure effect. Such global responses are difficult to interpret as direct responses to the presence of the layer without a corresponding dependence on the layer region. It is possible that the mere presence of the layer could modify the animals' behavior irrespective of their location. In this case, however, we would expect to see a dependency of the treatment effect on the animals' exposure to the layer. However, if we are not collecting enough time points before contact with the layer (pre-contact), we could miss the exposure effect. If the limited duration of the tracks limits the number of samples within the layer region, the location effect or dependency on the location, could be missed. In Table 4.18, the total number of data points, as well as the corresponding number of data points in-layer and pre-contact, are shown for each trial.

Table 4.18: The number of data points in the tracks for total length, in-layer portion, and pre-contact portion [mean (SE)]. The data were taken at 15 fps.

Sex	Experiment	Replicate	Total Track Length	In-Layer Track Length	Pre-Contact Track Length
Male	Control	1	281 (30)	118 (13)	76 (8)
		2	206 (21)	72 (7)	62 (6)
	Treatment	1	430 (66)	181 (28)	120 (18)
		2	401 (48)	189 (23)	88 (11)
Female	Control	1	189 (20)	85 (9)	61 (6)
		2	312 (41)	128 (17)	87 (12)
	Treatment	1	325 (30)	140 (13)	75 (7)
		2	290 (19)	116 (8)	70 (5)

In the future, I recommend using longer tracks, if possible, in order to minimize this effect as much as possible. Animals that consistently provide shorter tracks could be filmed at higher frame rates to better resolve local changes in behavior.

Lastly, there could be issues with the definition of the layer region, which is discussed at length in Section 4.2.3.

4.2.1 Strain Rate as a Mating Cue

We did not find clear evidence to support the idea that *H. shoshone* uses strain rate as a mating cue, despite observations made by Pender-Healy (2014) in which *H. shoshone* followed trail mimics with no female scent. However, there are several differences between these two experiments that could explain this observation. The trail mimics are made heavier than the surrounding fluid using dextran, a glucan molecule. Therefore, the animals could be reacting either to the density difference or the chemical signal of dextran rather than the shear strain rate at the edge of the trail

mimic. Harder (1968) has shown that *T. longicornis* respond to density differences without the presence of strain rate or salinity. In the case of a salinity difference in absence of a density difference, the animals were more or less evenly distributed between two layers of fluid (one of higher salinity, the other of lower salinity); when there were density differences with no salinity differences, the animals remained on the more dense (lower) layer.

Indeed, Yen (personal communication) has further observed than males appear to orient themselves dorsally to the trails, which could support the conjecture that the animals react to the chemical signal or density differences rather than to the shear strain rate. While the magnitudes of velocity in both the trail (2.9 - 12.3 mm/s) and the thin layer mimic are similar (0 - 6.7 mm/s), the size relative to the copepod as well the orientation relative to gravity is not; therefore, *H. shoshone* could be exhibiting a selective response in the case of the trail following experiments, showing a preferred size and/or orientation of hydromechanical cues. The time scale of the two experiments are very different as well; in the thin layer mimic experiment, the animals were exposed to the velocity gradient cue for 1 hour vs. a few minutes in the trail mimic experiments.

It is possible that the directionality of these cues is more important to the animals than previously thought; if so, a vertically oriented, downward facing Bickley jet could be used to investigate *H. shoshone* behavior response in a different configuration (see True et al. 2015). The vertical flow direction in such a configuration would match the dextran trails used by Yen et al. (2011) and Pender-Healy (2014). Further, horizontal gradients of vertical velocity may be more familiar to the animals since the lake mixes at least every night due to nighttime cooling. Hence, it is possible that the differences in behavior response between the trail-following trials and the current experiments are due to the orientation shift of the hydromechanical cues present in the treatment.

4.2.2 Response to Shear Layers: Freshwater vs. Marine

H. shoshone exhibited a global response to the thin layer treatment, decreasing its speed, increasing turning frequency, and increasing PVT from control to treatment. In contrast, a physiologically-similar marine copepod, *Calanus finmarchicus*, has been shown previously to react locally to the presence of thin layer cues via increased swimming speed and increased turn frequency from pre-contact to post-contact and increased proportional residence time from control to treatment (Woodson et al. 2007b). These results are shown in Figures 4.18, 4.19, and 4.20.

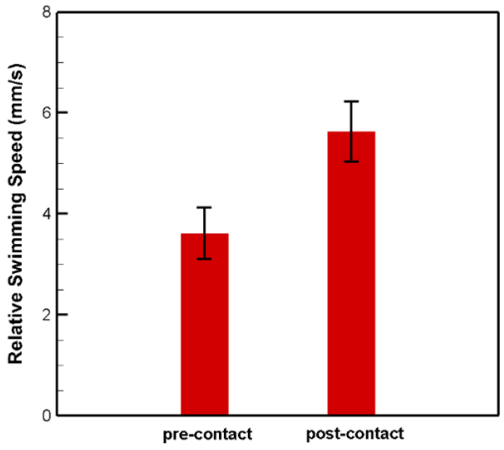

Figure 4.18: Relative swimming speed (mm/s) for *C. finmarchicus* pre-contact and post-contact with the layer in the thin layer treatment. The error bars are ± 1 SE. $n = 16$. Data from Woodson et al. (2007a).

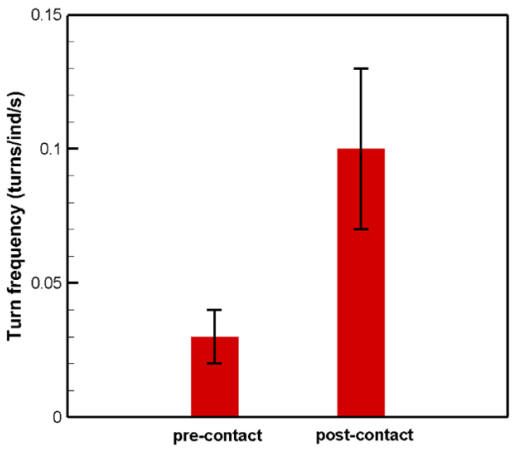

Figure 4.19: Turn frequency ($turns/ind/s$) for *C. finmarchicus* pre-contact and post-contact with the layer in the thin layer mimic. The error bars are ± 1 SE. $n = 16$. Data from Woodson et al. (2007b).

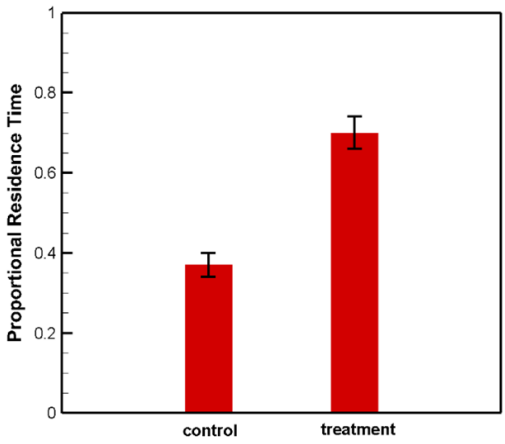

Figure 4.20: Proportional residence time (PRT) for *C. finmarchicus* in the thin layer treatment and control. The error bars are ± 1 SE. $n = 16$. Data from Woodson et al. (2007b).

The behavior response of *C. finmarchicus* is very clearly influenced by its exposure to the shear layer, exhbiting behaviors consistent with an area-restricted search

pattern (Woodson et al. 2007b).

H. shoshone and *C. finmarchicus* are morphologically similar, with body lengths varying around 3 - 4 *mm* in body length and planar setal arrays. Both copepods are cruising swimmers. However, these two copepods respond differently to the presence of shear layer cues. Whereas *C. finmarchicus* increases its speed, turning frequency, and PRT in accordance with an area-restricted search pattern (Woodson et al. 2007b), *H. shoshone* was observed to decrease its speed while increasing turning frequency and PVT, but not PRT. The most dramatic difference in behavior response is that the response of *H. shoshone* is not related to exposure to the layer region. Moreover, the freshwater copepods that were retrieved after the experiments were observed to be lethargic and in poor health; clearly the shear layer environment is not one in which these animals thrive.

Environment is a primary difference between these two animals. *C. finmarchicus* is a marine copepod that lives in the heavily stratified region of the ocean in which thin layers can set up and persist over several days (McManus et al. 2003), during which time zooplankton can congregate around these layers (Dekshenieks et al. 2001). In contrast, *H. shoshone* live in relatively shallow alpine lakes and ponds (Williams 2012) where free horizontal shear flows would be rare events (Slaymaker 1979). Most of the year, these lakes are frozen, thawing in late July and freezing again in early to late September. During the summer months, the only months during which these copepods are active, the lakes mix at least daily due to rapid nighttime cooling. These water bodies probably mix even more frequently since they are shallow enough that almost any breeze causes the entire water column to mix. In addition, these two animals hold very different positions within their respective food chains. Whereas *C. finmarchicus* is an herbivore and can be eaten by other zooplankton and fish, *H. shoshone* is an apex predator and carnivore in its environment, which has a relatively simple food web.

For *C. finmarchicus*, the presence of the physical cues of shear strain rate and velocity gradients acts an indicator that food and mates will be present, a benefit that these animals must weigh against the dangers of predators at these same locations. However, for the freshwater *H. shoshone*, there is no association between thin layer cues such as velocity gradients and the presence of food and mates due to the absence of persistent thin layer flow structures.

4.2.3 Shear Strain Rate Threshold

Although we did not observe a behavioral response by *H. shoshone* to the thin layer region, the shear strain rate threshold analysis (see Figures 4.4 and 4.5) suggested that the animals reacted to the presence of the shear layer. To further investigate this apparent contradiction of results, we took a female control data set and used the x and y positions from the digitized trajectories to find what the strain rate value would be at a given animal location for the horizontal Bickley jet. Both the applied shear strain rate field and the equivalent behavior response curve are shown in Figure 4.21.

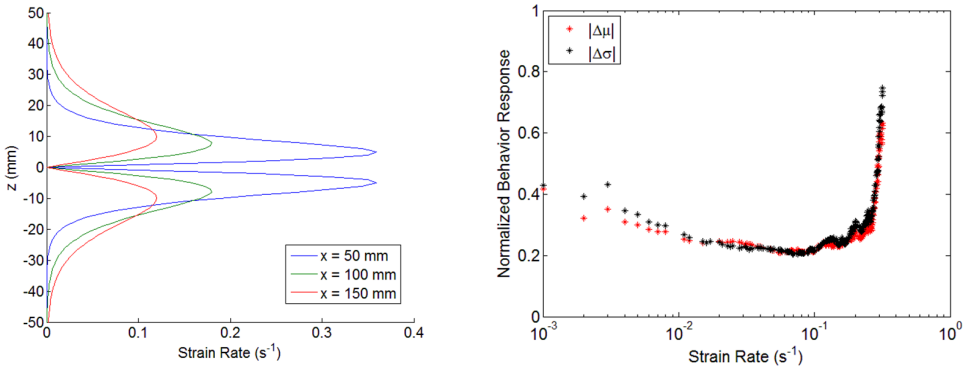

(a) (b)

Figure 4.21: (a) Shear strain rate field for the horizontal Bickley jet, and (b) hypothetical behavior response curve for the *H. shoshone* female control trajectories.

Indeed, the control case shows a similar response curve to the imposed shear strain rate field of the horizontal Bickley jet, yielding a shear strain rate threshold 0.2 s^{-1}. However, since this is a control set of digitized trajectories, the animals cannot be responding to the presence of shear strain rate. This result implies that this method alone cannot indicate whether or not a species reacts to a flow field.

To further explore how the velocity field applied to a data set affects the behavior response curve, several other velocity fields were synthetically applied to the digitized trajectories for the female control experiment. A vertical Bickley jet was used to investigate the effect of orientation on the response curve. The result is shown in Figure 4.22. Again, the behavior response curve yields a shear strain rate threshold of 0.1 s^{-1}. Thus, the orientation of the imposed Bickley jet does not seem to change the hypothetical behavior response curve.

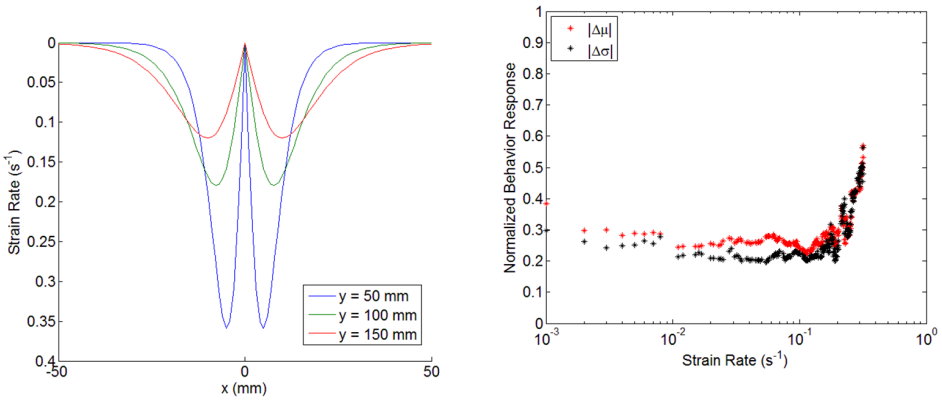

(a) (b)

Figure 4.22: (a) Shear strain rate field for the vertical Bickley jet, and (b) hypothetical behavior response curve for the *H. shoshone* female control trajectories.

The flow field of the Bickley jet results in a sharp drop in shear strain rate near the jet centerline. If a flow field is applied such that the maximum strain rate is maintained across the peaks, as shown in Figure 4.23a, the response curve yielded

is that shown in Figure 4.23b. The behavior response curve is seemingly unchanged from the original control response curve shown in Figure 4.21, yielding the same shear strain rate threshold of 0.1 s^{-1}.

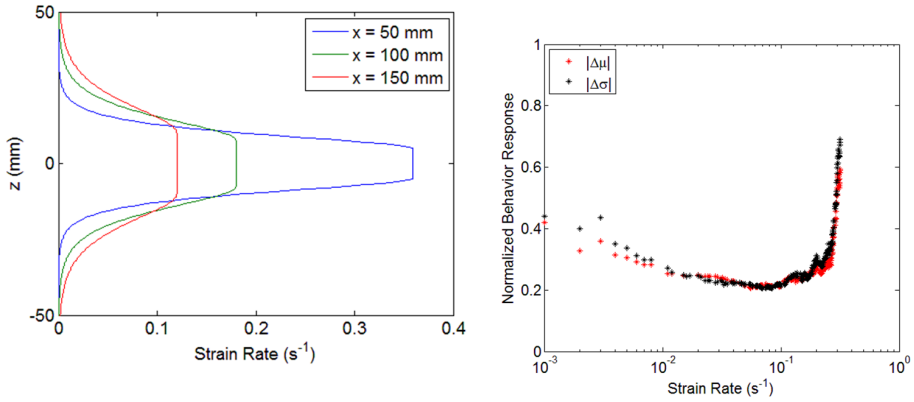

(a) (b)

Figure 4.23: (a) Shear strain rate field for horizontal Bickley jet with constant shear strain rate between peaks, and hypothetical behavior response curve for the *H. shoshone* female control trajectories.

Lastly, I examined whether the decay in shear strain rate downstream influenced the behavior response curve. The result is shown in Figure 4.24, where a hyperbolic tangent velocity profile was applied to the control data set. The hyperbolic tangent velocity profile does not exhibit the decay in shear strain rate in the streamwise direction that is present in the Bickley jet. Therefore we can isolate the effect of the jet area relative the total area of the observation window (for these experiments, the jet area was 33% of the total observation area) and examine how the behavior response curve is affected.

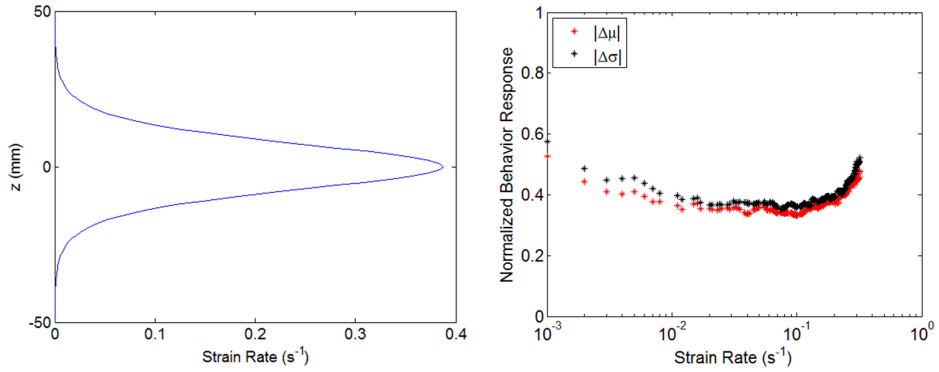

(a) (b)

Figure 4.24: (a) Shear strain rate field for the hyperbolic tangent velocity profile, and (b) hypothetical behavior response curve for the *H. shoshone* female control trajectories.

The behavior response curve for the hyperbolic tangent velocity profile shows no threshold. There is a slight turning up for shear strain rate values greater than 0.2 s^{-1}, but this upturn is similar in magnitude to that at the smallest values of strain rate. Ultimately, this slight change in slope is not strong enough to indicate there is a behavior response. This result implies that there is an effect of the restricted area of the Bickley jet on the behavior response curve (as shown in Figures 4.21, 4.22, and 4.23) but that this effect is mostly due to the downstream decease of the strain rate magnitude rather than the restriction of the layer to the middle third of the observation window. From Figure 4.24, we can see that when this decaying of strain rate is removed, the behavior response curve flattens significantly and no longer exhibits a rapid change in slope at any particular strain rate value, which would denote a threshold.

All jets will decay with distance from the jet nozzle, and restricting the window in either the streamwise or cross-stream directions would only further limit the number of encounters with high or low strain rate values. The Bickley jet is notoriously finicky

(Andrade 1939), and it is already running in the transitionally stable laminar flow regime ($Re_j = 50$) near the maximum limit of stability ($Re_j = 60$, Sato and Sakao 1964). Lower Reynolds numbers would only exacerbate the problem by having the jet decay even more quickly with streamwise distance, not to mention that the velocities might be too low to create relevant hydromechanical signals.

All three Bickley jet cases yielded a shear strain rate threshold that basically corresponded to the edge of the jet layer, as seen in Figure 2.2 (the value of 0.1 s^{-1} is the green color contour). A value corresponding to the edge of the jet layer is highlighted in the behavior response curve because it is a value of strain rate that is found commonly in the observation region. As the strain rate value increases, the trajectory encounters with such values become more rare, causing larger differences in mean and standard deviations below and above these strain rate values. This larger difference gives the false impression in the strain rate threshold analysis that the animals are reacting at certain shear strain rate value.

These results imply that the process of comparing the means and standard deviations above and below different shear strain rate values is overwrought, and that simply picking a value corresponding the edge of the jet layer and comparing data inside and outside this region is just as effective. Alternatively, one could compare the behavior response curve of the control specimen to that of the animals that were exposed to the shear layer and look for the shear strain rate value at which these two curves differ. To examine the differences between the two curves, one could fit a polynomial through each curve and compare the two polynomials, or one could plot them together to look for a shift along the shear strain rate axis. Of course, in order to use this method one would need an analytical expression or fine-resolution PIV of the flow field in order to synthetically apply the flow field to the digitized trajectories of the control experiments.

CHAPTER V

CONCLUSION

In previous work, marine copepods have been shown to behaviorally respond to vertical gradients of horizontal velocity and aggregate around thin layers (Woodson et al. 2005; Woodson et al. 2007a; Woodson et al. 2007b; Woodson et al. 2014; True et al. 2015). Thin layers are vertically thin, horizontally expansive layers in the ocean that have high productivity and are found in nearly all marine environments. Within marine environments, the hydromechanical cues of velocity gradients and shear strain rate rank in a cue hierarchy that indicate where food and mates are likely to be found. The current thesis explores the question of whether freshwater copepods similarly respond to shear strain rate cues associated with environmental structure.

Alpine lakes in particular are excellent candidates for study and could serve as sentinels of climate change. In these environments, changes in hydrology, such as changes in snowpack, could be linked with change to community structure and population decline (or incline). One freshwater copepod, *Hesperodiaptomus shoshone*, has previously been seen to thrive in years of low snowpack and decline in years of high snowpack due to an invader species (Williams 2012). This connection, as well as the physiological response of *H. shoshone* to ultraviolet radiation flux in the form of protective pigment, make it an interesting species to study in connection to climate change.

Previous studies indicate that *H. shoshone* may use trail-following in order to improve mating success (Yen et al. 2011; Pender-Healy 2014); however, there are several cues present in the trail mimics that researchers use to isolate the trail from the physical presence of a female zooplankton. These cues include chemical cues

of the female pheromone, the heavy-weight molecular sugar used to make the trails negatively buoyant, and the hydromechanical cues of shear strain rate at the edges of the trail. In the experiments supporting this thesis, the hydromechanical cues are separated from other cues in the laboratory using a laminar, planar free jet (the Bickley jet) in a recirculating system. This system has been shown to mimic the characteristics of thin layers (True 2014).

Freshwater copepod *H. shoshone* showed a significant treatment effect, but did not exhibit a behavior response to the location within or exposure to thin layer velocity gradients. This conclusion is based on the lack of significant difference in the following parameters (for in-layer vs. out-of-layer and pre-contact vs. post-contact analyses): relative swimming speed, turning frequency, net-to-gross-displacement ratio, proportional residence time, proportional vicinity time, and body orientation. In contrast, the marine copepod *Calanus finmarchicus*, which is very similar physiologically, showed a strong response to the same stimuli (Woodson et al. 2007b). The difference of reaction between these two species may be explained by ecology and environment considerations. Because the freshwater copepod lives in alpine lakes that mix frequently (Slaymaker 1979), there is no opportunity for thin layer flow structures to form and persist. Therefore, there is no association among flow structure, food, and mates in this environment.

We found no clear evidence that strain rate cue plays a role in mating behaviors. Pender-Healy (2014) observed increasing swimming speeds in males in response to the trail mimics, while the copepods in our experiments decreased their speed in response to the presence of velocity gradients. While there were significant sex effects in turning frequency, along with significant or marginally significant treatment effects, we cannot say with certainty that these effects are due specifically to the shear layer.

The method used to identify the shear strain rate threshold cannot indicate that a reaction took place. This method appears to simply identify a value of shear strain

rate near the edge of the jet layer. In the future, comparisons could be made between control and treatment behavior response curves. Alternatively, one could simply pick a shear strain rate that corresponds to a value near the edge of the layer and use that threshold to make statistical comparisons between in-layer and out-of-layer as well as pre-contact and post-contact data.

APPENDIX A

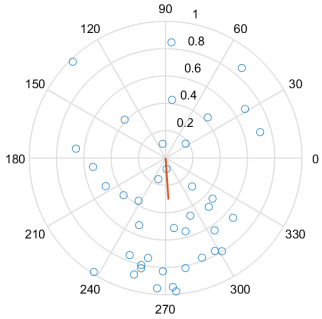

(a) Male treatment, replicate 1

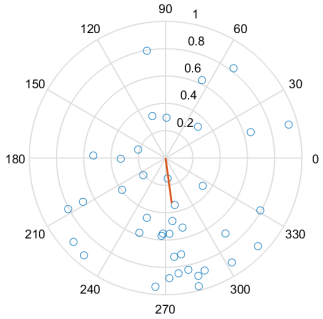

(b) Male treatment, replicate 2

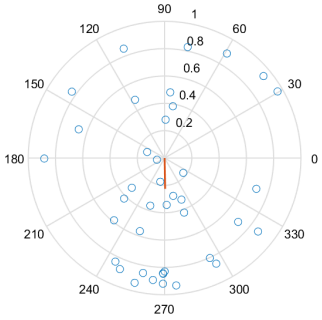

(c) Male control, replicate 1

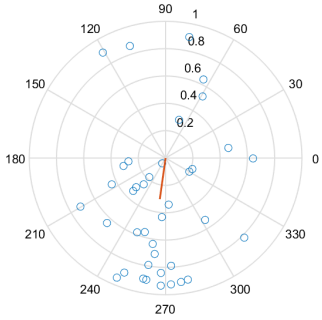

(d) Male control, replicate 2

Figure A.1: Distributions of body orientation for *H. shoshone* males. The open circles show the individual copepod mean angle, and the orange vector shows the mean angle of the population. The distance from the center indicates how strong the preference for a particular direction is. There is no difference between the replicates, and there is no difference between treatment and control.

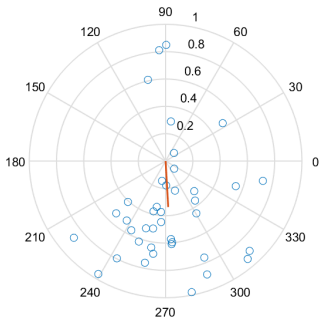

(a) Female treatment, replicate 1

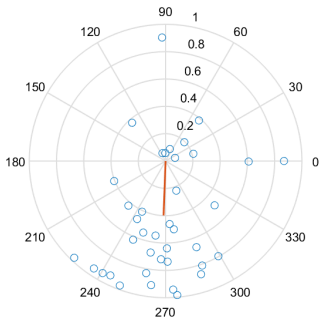

(b) Female treatment, replicate 2

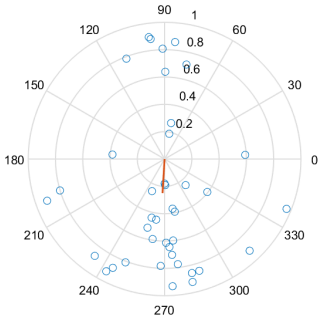

(c) Female control, replicate 1

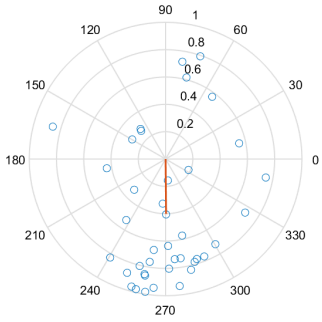

(d) Female control, replicate 2

Figure A.2: Distributions of body orientation for *H. shoshone* females. The open circles show the individual copepod mean angle, and the orange vector shows the mean angle of the population. The distance from the center indicates how strong the preference for a particular direction is. There is no difference between the replicates, and there is no difference between treatment and control.

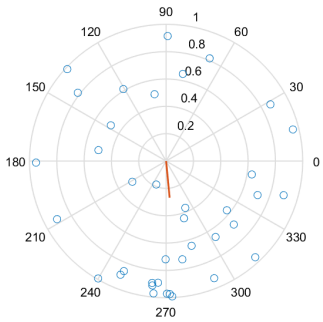

(a) In-layer

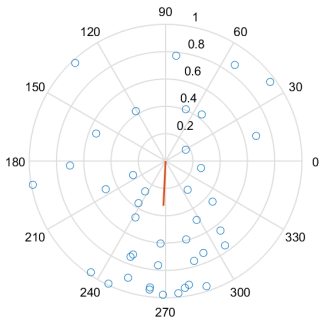

(b) Out-of-layer

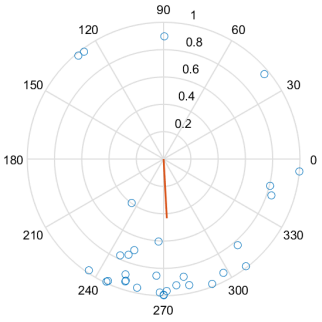

(c) Pre-contact

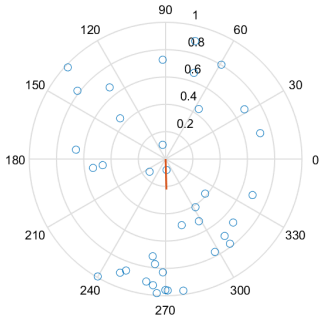

(d) Post-contact

Figure A.3: Distributions of body orientation for *H. shoshone* male treatment, replicate 1. The open circles show the individual copepod mean angle, and the orange vector shows the mean angle of the population. The distance from the center indicates how strong the preference for a particular direction is. There is no difference between in-layer and out-of-layer, and there is no difference between pre-contact and post-contact.

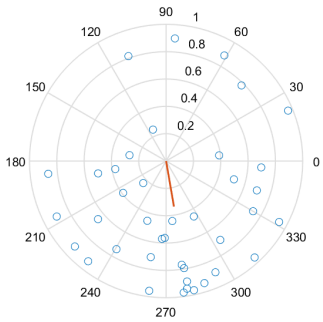

(a) In-layer

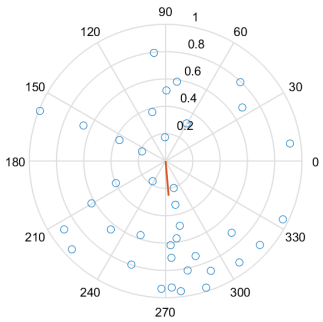

(b) Out-of-layer

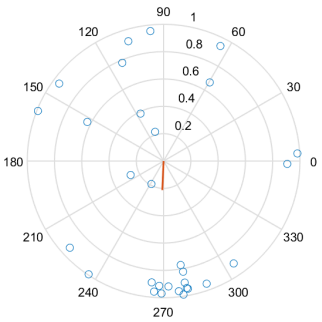

(c) Pre-contact

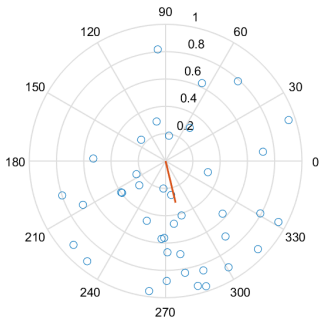

(d) Post-contact

Figure A.4: Distributions of body orientation for *H. shoshone* male treatment, replicate 2. The open circles show the individual copepod mean angle, and the orange vector shows the mean angle of the population. The distance from the center indicates how strong the preference for a particular direction is. There is no difference between in-layer and out-of-layer, and there is no difference between pre-contact and post-contact.

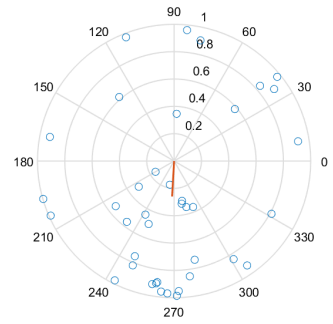

(a) In-layer

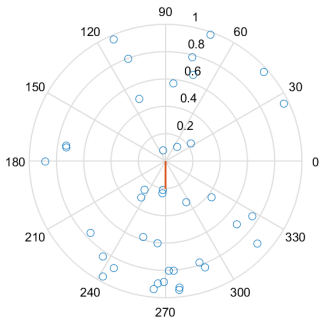

(b) Out-of-layer

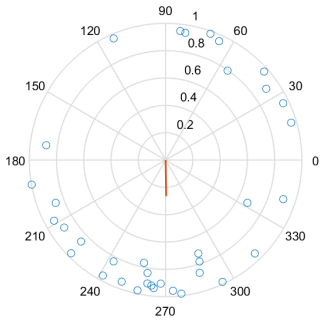

(c) Pre-contact

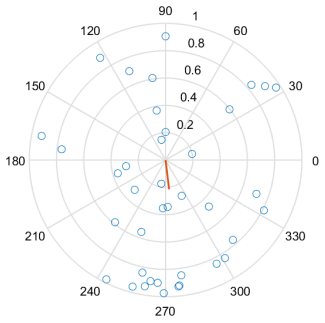

(d) Post-contact

Figure A.5: Distributions of body orientation for *H. shoshone* male control, replicate 1. The open circles show the individual copepod mean angle, and the orange vector shows the mean angle of the population. The distance from the center indicates how strong the preference for a particular direction is. There is no difference between in-layer and out-of-layer, and there is no difference between pre-contact and post-contact.

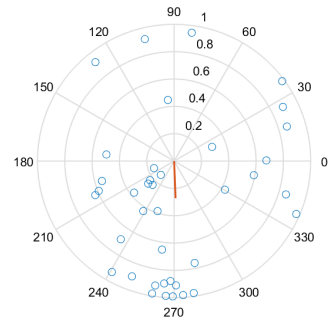

(a) In-layer

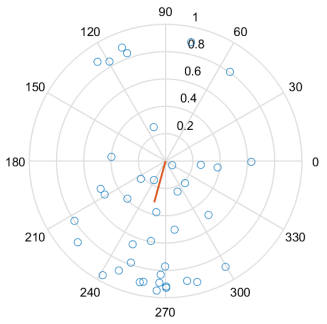

(b) Out-of-layer

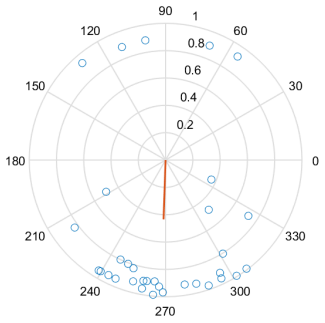

(c) Pre-contact

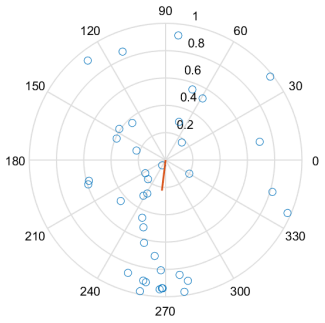

(d) Post-contact

Figure A.6: Distributions of body orientation for *H. shoshone* male control, replicate 2. The open circles show the individual copepod mean angle, and the orange vector shows the mean angle of the population. The distance from the center indicates how strong the preference for a particular direction is. There is no difference between in-layer and out-of-layer, and there is no difference between pre-contact and post-contact.

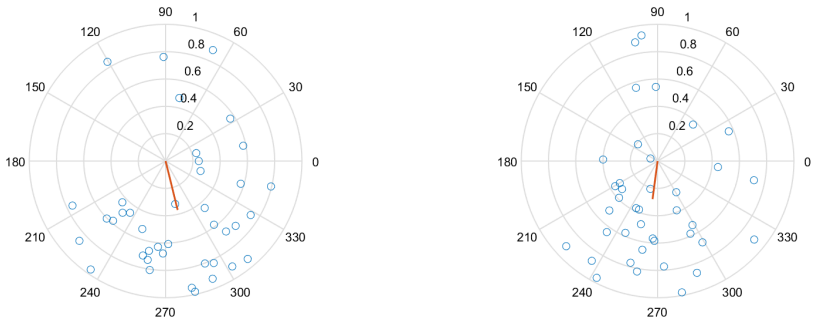

(a) In-layer

(b) Out-of-layer

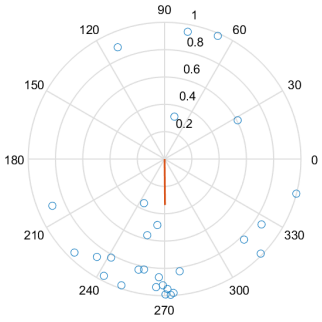

(c) Pre-contact

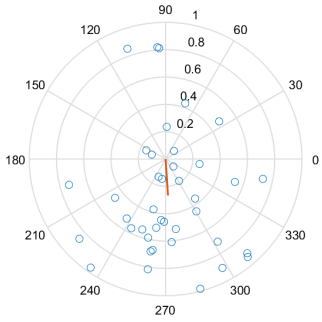

(d) Post-contact

Figure A.7: Distributions of body orientation for *H. shoshone* female treatment, replicate 1. The open circles show the individual copepod mean angle, and the orange vector shows the mean angle of the population. The distance from the center indicates how strong the preference for a particular direction is. There is no difference between in-layer and out-of-layer, and there is no difference between pre-contact and post-contact.

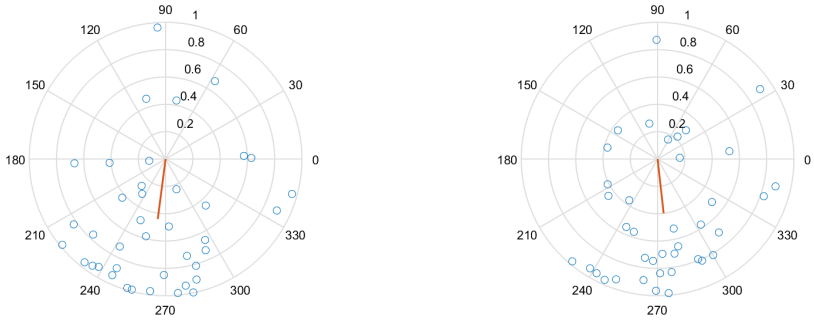

(a) In-layer

(b) Out-of-layer

(c) Pre-contact

(d) Post-contact

Figure A.8: Distributions of body orientation for *H. shoshone* female treatment, replicate 2. The open circles show the individual copepod mean angle, and the orange vector shows the mean angle of the population. The distance from the center indicates how strong the preference for a particular direction is. There is no difference between in-layer and out-of-layer, and there is no difference between pre-contact and post-contact.

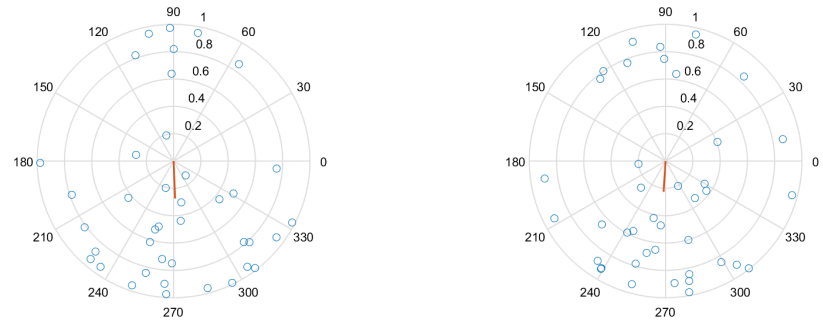

(a) In-layer

(b) Out-of-layer

(c) Pre-contact

(d) Post-contact

Figure A.9: Distributions of body orientation for *H. shoshone* female control, replicate 1. The open circles show the individual copepod mean angle, and the orange vector shows the mean angle of the population. The distance from the center indicates how strong the preference for a particular direction is. There is no difference between in-layer and out-of-layer, and there is no difference between pre-contact and post-contact.

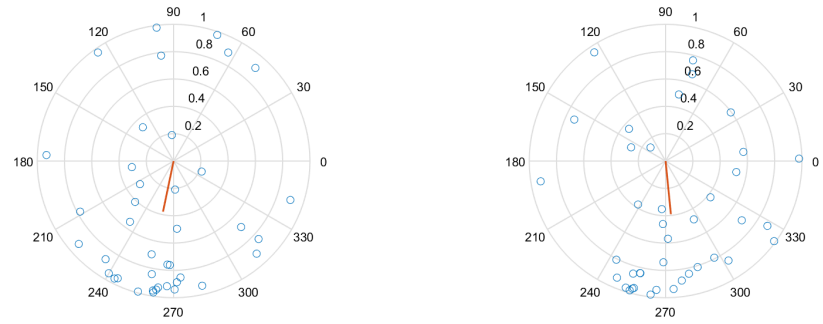

(a) In-layer

(b) Out-of-layer

(c) Pre-contact

(d) Post-contact

Figure A.10: Distributions of body orientation for *H. shoshone* female control, replicate 2. The open circles show the individual copepod mean angle, and the orange vector shows the mean angle of the population. The distance from the center indicates how strong the preference for a particular direction is. There is no difference between in-layer and out-of-layer, and there is no difference between pre-contact and post-contact.

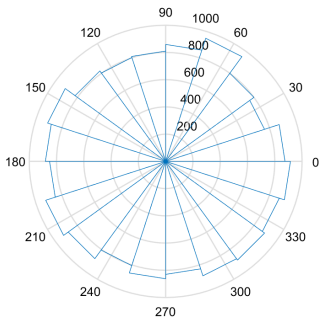

(a) Male treatment, replicate 1

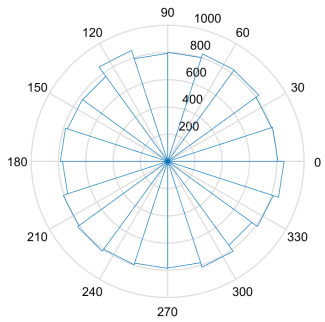

(b) Male treatment, replicate 2

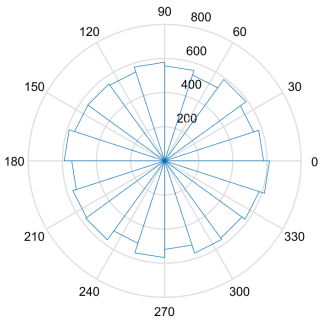

(c) Male control, replicate 1

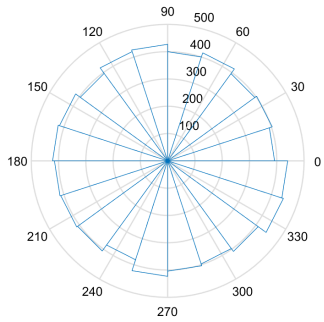

(d) Male control, replicate 2

Figure A.11: Histograms of body orientation for *H. shoshone* males. The width of each wedge is the bin width, equal to 18°, and the length of the wedge indicates the number of observations in that angle range. There is no difference between the replicates, and there is no difference between treatment and control.

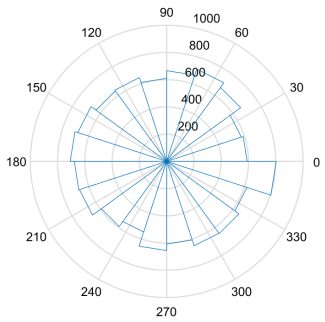

(a) Female treatment, replicate 1

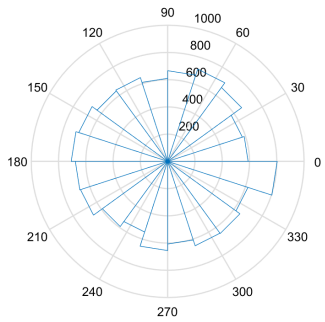

(b) Female treatment, replicate 2

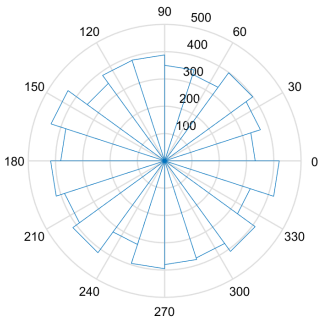

(c) Female control, replicate 1

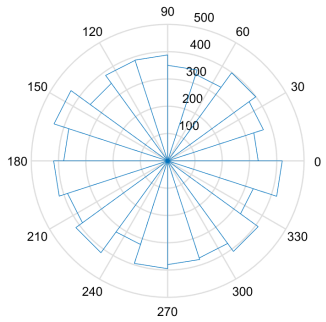

(d) Female control, replicate 2

Figure A.12: Histograms of body orientation for *H. shoshone* males. The width of each wedge is the bin width, equal to 18°, and the length of the wedge indicates the number of observations in that angle range. There is no difference between the replicates, and there is no difference between treatment and control.

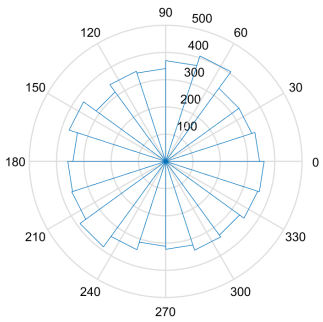

(a) In-layer

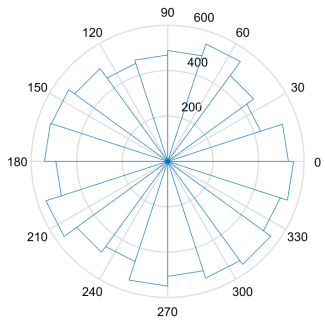

(b) Out-of-layer

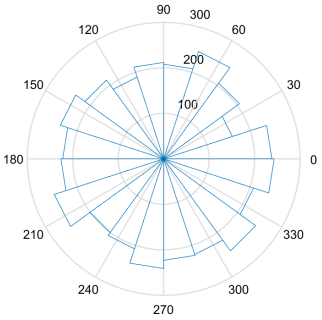

(c) In-layer

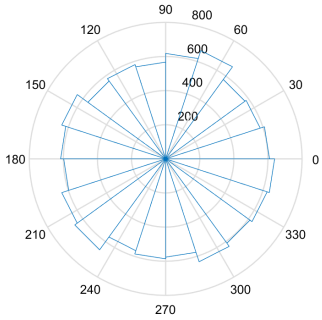

(d) Out-of-layer

Figure A.13: Histograms of body orientation for *H. shoshone* male treatment, replicate 1. The width of each wedge is the bin width, equal to 18°, and the length of the wedge indicates the number of observations in that angle range. There is no difference between in-layer and out-of-layer, and there is no difference between pre-contact and post-contact.

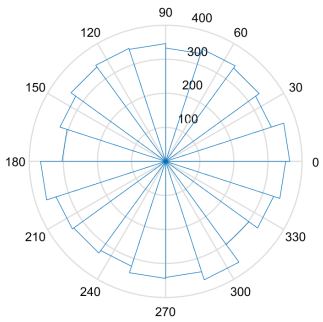

(a) In-layer

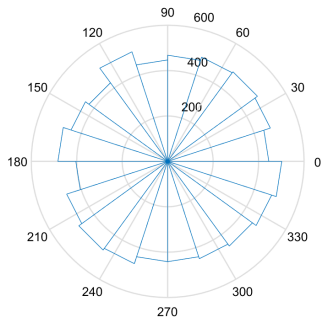

(b) Out-of-layer

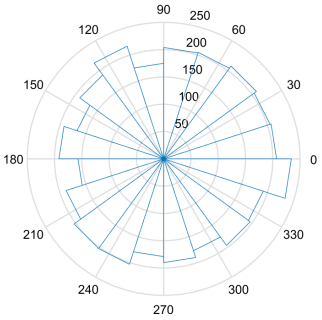

(c) In-layer

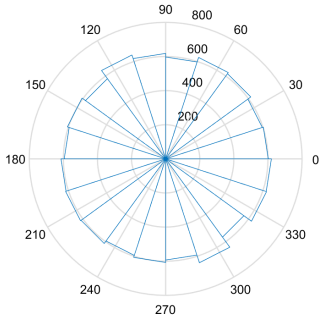

(d) Out-of-layer

Figure A.14: Histograms of body orientation for *H. shoshone* male treatment, replicate 2. The width of each wedge is the bin width, equal to 18°, and the length of the wedge indicates the number of observations in that angle range. There is no difference between in-layer and out-of-layer, and there is no difference between pre-contact and post-contact.

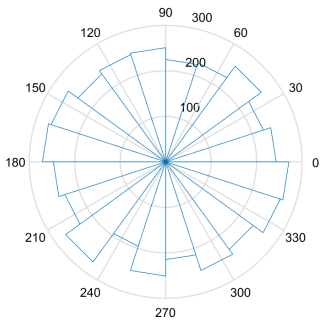

(a) In-layer

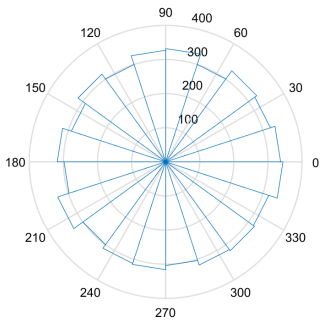

(b) Out-of-layer

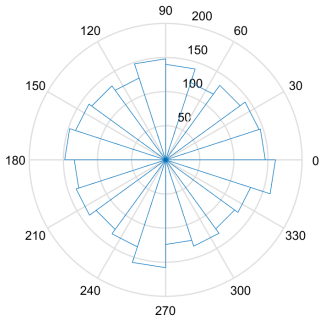

(c) In-layer

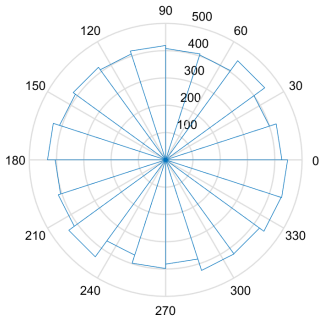

(d) Out-of-layer

Figure A.15: Histograms of body orientation for *H. shoshone* male control, replicate 1. The width of each wedge is the bin width, equal to 18°, and the length of the wedge indicates the number of observations in that angle range. There is no difference between in-layer and out-of-layer, and there is no difference between pre-contact and post-contact.

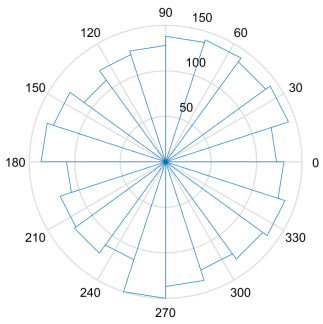

(a) In-layer

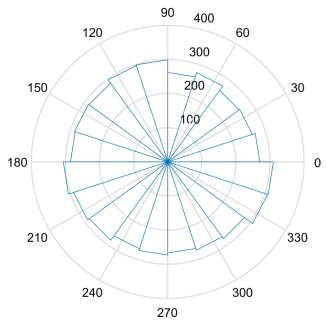

(b) Out-of-layer

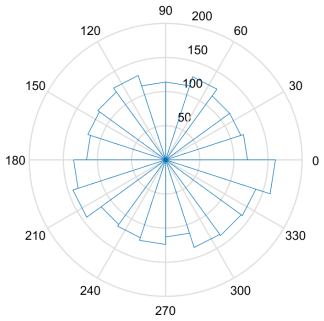

(c) In-layer

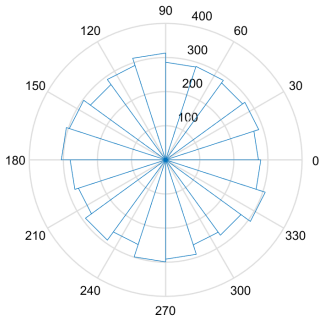

(d) Out-of-layer

Figure A.16: Histograms of body orientation for *H. shoshone* male control, replicate 2. The width of each wedge is the bin width, equal to 18°, and the length of the wedge indicates the number of observations in that angle range. There is no difference between in-layer and out-of-layer, and there is no difference between pre-contact and post-contact.

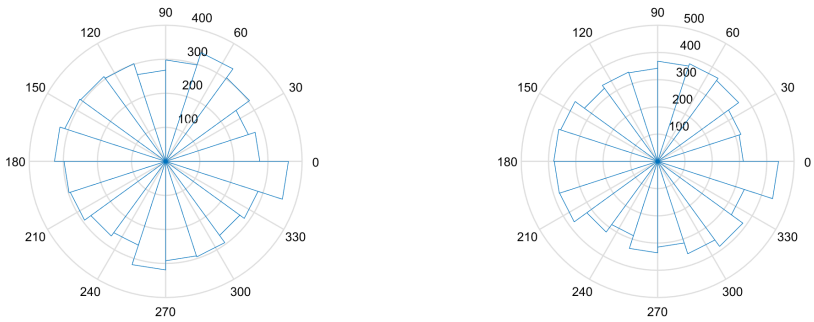

(a) In-layer

(b) Out-of-layer

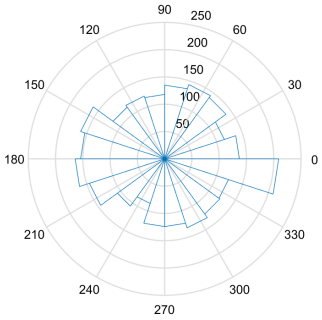

(c) In-layer

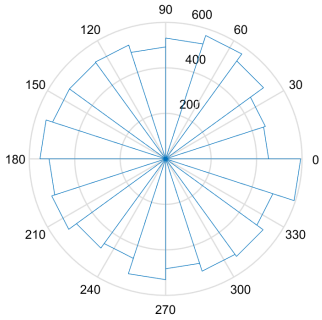

(d) Out-of-layer

Figure A.17: Histograms of body orientation for *H. shoshone* female treatment, replicate 1. The width of each wedge is the bin width, equal to 18°, and the length of the wedge indicates the number of observations in that angle range. There is no difference between in-layer and out-of-layer, and there is no difference between pre-contact and post-contact.

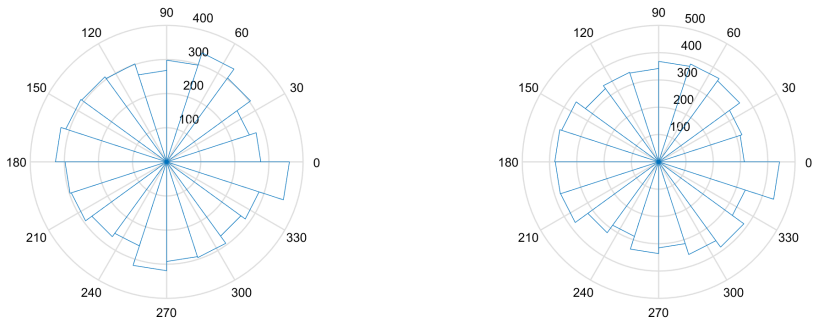

(a) In-layer

(b) Out-of-layer

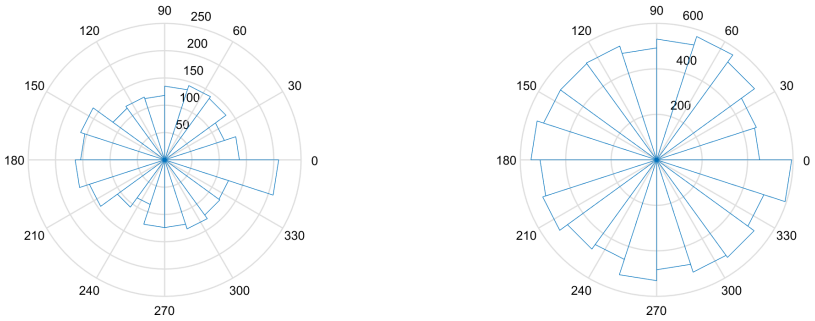

(c) In-layer

(d) Out-of-layer

Figure A.18: Histograms of body orientation for *H. shoshone* female treatment, replicate 2. The width of each wedge is the bin width, equal to 18°, and the length of the wedge indicates the number of observations in that angle range. There is no difference between in-layer and out-of-layer, and there is no difference between pre-contact and post-contact.

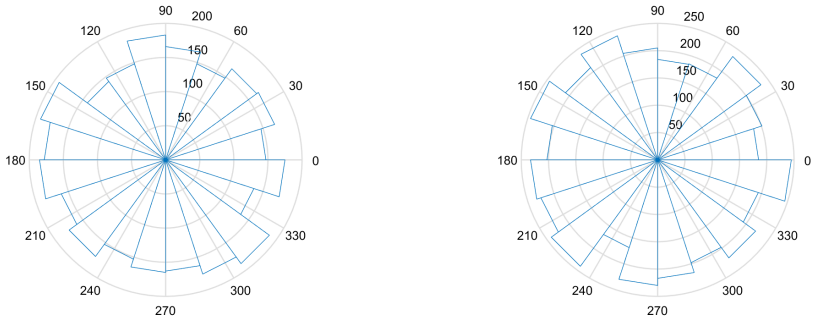

(a) In-layer

(b) Out-of-layer

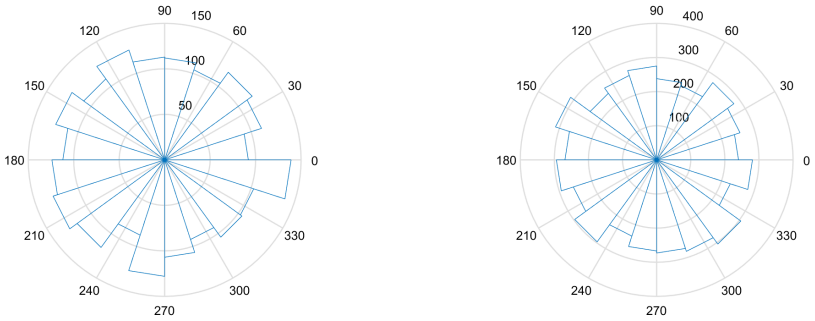

(c) In-layer

(d) Out-of-layer

Figure A.19: Histograms of body orientation for *H. shoshone* female control, replicate 1. The width of each wedge is the bin width, equal to 18°, and the length of the wedge indicates the number of observations in that angle range. There is no difference between in-layer and out-of-layer, and there is no difference between pre-contact and post-contact.

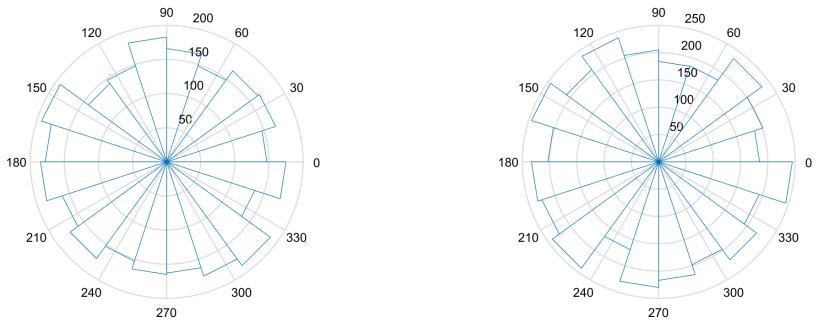

(a) In-layer (b) Out-of-layer

(c) In-layer (d) Out-of-layer

Figure A.20: Histograms of body orientation for *H. shoshone* female control, replicate 2. The width of each wedge is the bin width, equal to 18°, and the length of the wedge indicates the number of observations in that angle range. There is no difference between in-layer and out-of-layer, and there is no difference between pre-contact and post-contact.

References

R. Adrian, C.M. O'Reilly, H. Zagarese, S.B. Baines, and *et. al* D.O. Hessen. Lakes as sentinels of climate change. *Limnol Oceanogr*, 54:2283–2297, 2009.

E.C. Andrade. The velocity distribution in a liquid-into-liquid jet. part 2: The plane jet. *Proc Phys Soc*, 51:784–793, 1939.

W.G. Bickley. The plane jet. *Philosophical Magazine*, 23:727–731, 1937.

O.M. Cheriton, M.A. McManus, M.T. Stacey, and J.V. Steinbuck. Physical and biological controls on the maintenance and dissipation of a thin phytoplankton layer. *Mar Ecol Prog Ser*, 378:55–69, 2009.

M.J. Dagg and J.T. Turner. The impact of copepod grazing on the phytoplankton of georges bank and the new york bight. *Can J Fish Aq Sci*, 39:979–990, 1982.

M.M. Dekshenieks, P.L. Donaghay, J.M. Sullivan, J.E.B. Rines, T.R. Osborn, and M.S. Twardowski. Temporal and spatial occurrence of thin phytoplankton layers in relation to physical processes. *Mar Ecol Prog Ser*, 223:61–71, 2001.

P.G. Drazin and W.H. Reid. *Hydrodynamic stability*. Cambridge University Press, United Kingdom, 1981.

J. T. Enright and W. M. Hamner. Vertical diurnal migration and endogenous rhythmicity. *Science*, 157:937941, 1967.

D.M. Fields. Orientation affects the sensitivity of *Acartia tonsa* to fluid mechanical signals. *Marine Biology*, 157:505–514, 2010.

D.M. Fields, D.S. Shaeffer, and M.J. Weissburg. Mechnical and neural responses from the mechanosensory hairs on the antennule of *Gaussia princeps*. *Mar Ecol Prog Ser*, 227:173–186, 2002.

H.B. Fischer, E.J. List, R.C.Y. Koh, J. Imberger, and N.H. Brooks. *Mixing in Inland and Coastal Waters*. Academic Press, San Diego, 1979.

P.J.S. Franks. Thin layers of phytoplankton: a model of formation by near-inertial wave shear. *Deep Sea Res I*, 42:75–91, 1995.

Ian Gardiner. *Hesperodiaptomus shoshone* (Copepod), 2010. URL `http://linnet.geog.ubc.ca/efauna/`.

L.A. Hansson, S. Hylander, and R. Sommaruga. Escape from {UV} threates in zooplankton: a cocktail of behavior and protective pigmentation. *Ecology*, 88: 1932–1939, 2007.

W. Harder. Reaction of plankton organisms to water stratification. *Limnol Oceanogr*, 13:156–168, 1968.

T.L. Hedrick. Software techniques for two- and three-dimensional kinematic measurements of biological and biomimetic systems. *Bioinspiration and Biomimetics*, 3(3): 034001, 2008.

R. Holzman and P.C. Wainwright. How to surprise a copepod: Strike kinematics reduce hydrodynamic disturbance and increase stealth of suction-feeding fish. *Limnol Oceanogr*, 54:22012212, 2009.

H.J. Hussein. Evidence of local axisymmetry in the small scales of a turbulent planar jet. *Phys. Fluids*, 2:400–412, 1990.

G.E. Hutchinson. *A Treatise on Limnology*, volume 1. Wiley and Sons, New York, 1957.

X. Jiang, Y. Tang, D.J. Lonsdale, , and C.J. Gobler. Deleterious consequences of a red tide dinoflagellate *Cochlodinium polykrikoides* for the calanoid copepod *Acartia tonsa*. *Mar Ecol Prog Ser*, 390:105–116, 2009.

K. Kessler, R.S. Lockwood, and C.E. Williamson. Vertical distribution of zooplankton in subalpine and alpine lakes: Ultraviolet radiation, fish predation, and the transparency-gradient hypotehsis. *Limnol Oceanogr*, 53:2374–2382, 2008.

T. Kiørboe and A.W. Visser. Predator and prey perception in copepods due to hydromechanical signals. *Mar Ecol Prog Ser*, 179:81–95, 1999.

T. Kiørboe, E. Saiz, and A.W. Visser. Hydrodynamic signal perception in the copepod *Acartia tonsa*. *Mar Ecol Prog Ser*, 179:97–111, 1999.

A.M. Kramer, O. Sarnelle, and J. Yen. The effect of mating behavior and temperature variation on the critical population density of a freshwater copepod. *Limnol Oceanogr*, 56:705–715, 2011.

P. K. Kundu, I. M. Cohen, and D. R. Dowling. *Fluid Mechanics*. Elsevier Academic Press, Waltham, MA, 2012.

T. Lyman. The west lobe of the west grasshopper glacier, 2012. URL `http://ravallirepublic.com/image_093bf551-ffb3-5805-9149-b81fbeb4f1a7.html`.

E.J. Maly. The influence of predation on the adult sex ratios of two copepod species. *Limnol Oceanogr*, 15:566–573, 1970.

E.J. Maly. Some factors influencing size of diaptomus shoshone. *Limnol Oceanogr*, 23:835–837, 1978.

J. Mauchline. *The Biology of Calanoid Copepods*. Elsevier Academic Press, San Diego, CA, 1998.

Daniel Mayor. *Calanus finmarchicus*, 2009. URL `http://www.coastalwiki.org/wiki/File:Calanus_finmarchicus.jpg`.

M.A. McManus, A.L. Alldredge, A.H. Barnard, E. Boss, and et al. Characteristics, distribution and persistence of thin layers over a 48 hour period. *Mar Ecol Prog Ser*, 261:1–19, 2003.

R.D. Mehta and P. Bradshaw. Design rules for small low speed wind tunnels. *Aeronautical Journal*, 83:443–449, 1979.

A. Nihongi, S.B. Lovern, and J.R. Strickler. Mate-searching behaviors in the freshwater calanoid copepod leptodiaptomus ashlandi. *Journal of Marine Systems*, 49: 65–74, 2004.

B.R. Parker, R.D. Vinebrook, and D.W. Schindler. Recent climate extremes alter alpine lake ecosytems. *Proceedings of the National Academy of Sciences*, 105:12927–12931, 2008.

L. Pender-Healy. Tracking response of the freshwater copepod hesperodiaptomus shoshone: Importance of hydrodynamic features. Master's thesis, Georgia Institute of Technology, Atlanta, GA, 2014.

R.W. Pennak. Diurnal movements of zooplankton organisms in some colorado mountain lakes. *Ecology*, 25:387–403, 1944.

J.P. Ryan, M.A. McManus, J.D. Paduan, and F.P. Chavez. Phytoplankton thin layers caused by shear in frontal zones of a coastal upwelling system. *Mar Ecol Prog Ser*, 354:21–34, 2008.

H. Sato and F. Sakao. An experimental investigation of the instability of a two-dimensional jet a low reynolds numbers. *J Fluid Mech*, 20:337–352, 1964.

H.O. Slaymaker. Alpine hydrology. In Jack D. Ives, editor, *Arctic and Alpine Environments*, pages 131–158. Harper and Row Publishers, London, 1979.

R. Sommaruga. The role of solar {UV} radiation in the ecology of alpine lakes. *Journal of Photochemistry and Photobiology B: Biology*, 62:35–42, 2001.

W.G. Sprules. Effects of size-selective predation and food competition on high altitude zooplankton communities. *Ecoloy*, 53:375–386, 1972.

J.R. Strickler and G. Balazsi. Planktonic copepods reacting selectively to hydrodynamic distrubances. *Phil Tras R Soc*, 362:1942–1958, 2007.

A.C. True. Ecological engines: Finescale hydrodynamic and chemical cues, zooplankton behavior, and implications for nearshore marine ecosystems. Master's thesis, Georgia Institute of Technology, Atlanta,GA, 2014.

A.C. True, D.R. Webster, M.J. Weissburg, J. Yen, and A. Genin. Patichiness and depth-keeping of copepods in response to simulated frontal flows. *Mar Ecol Prog Ser*, 539:65–76, 2015.

L.A. van Duren. Reading the copepod personal ads: increasing encounter probability with hydromechanical signals. *Phil Trans R Soc Lond B Biol Sci*, 353:691–700, 1998.

E.H. Williams. Long term effects of climate on two pond predators. *The American Midland Naturalist*, 167:336–343, 2012.

K. Wishner, E. Durbin, A. Durbin, M. MacCaulay, H. Winn, , and R. Kenney. Copepod patches and right whales in the great south channel off new england. *Bull Mar Sci*, 43:825–844, 1988.

C.B. Woodson, D.R. Webster, M.J. Weissburg, and J. Yen. Response of copepods to physical gradients associated with structure in the ocean. *Limnol Oceanogr*, 50: 1552–1564, 2005.

C.B. Woodson, D.R. Webster, M.J. Weissburg, and J. Yen. Cue hierarchy and foraging in calanoid copepods: ecological implications of oceanographic structure. *Mar Ecol Prog Ser*, 330:163–177, 2007a.

C.B. Woodson, D.R. Webster, M.J. Weissburg, and J. Yen. The prevalence and implications of copepod behavioral responses to oceanographic gradients and biological patchiness. *Integr Comp Biol*, 47:831–846, 2007b.

C.B. Woodson, D.R. Webster, and A.C. True. Copepod behavior: Oceanographic cues, distributions, and trophic interactions. In L. Seuront, editor, *Copepods: Diversity, Habitat, and Behavior*, pages 215–253. Nova Publishers, New York, 2014.

J. Yen and D.M. Fields. Escape responses of *Acartia hudsonica* (copepoda) nauplii from the flow field of temora longicornis (copepoda). *Archive Hydrobiol*, 36:123–134, 1992.

J. Yen, P.H. Lenz, D.V. Gassie, and D.K. Hartline. Mechanoreception in marine copepods: Electrophysical studies on the first antenae. *Journal of Plankton Research*, 14:495–512, 1992.

J. Yen, J.K. Sehn, K. Catton, A. Kramer, and O. Sarnelle. Pheremone trail following in three dimensions by the freshwater copepod hesperodiaptomus shoshone. *Journal of Plankton Research*, 33:907–916, 2011.

J.H. Zar. *Biostatistical Analysis*. Prentice Hall, Upper Saddle Hall, NJ, 4th edition edition, 1999.